

行政院國家科學委員會專題研究計畫 成果報告

多功能微液滴操控平台與陣列式反應器系統的開發 研究成果報告(精簡版)

計畫類別：個別型
計畫編號：NSC 99-2628-E-007-028-
執行期間：99年08月01日至100年07月31日
執行單位：國立清華大學工程與系統科學系

計畫主持人：蘇育全

計畫參與人員：碩士班研究生-兼任助理人員：張勝智
碩士班研究生-兼任助理人員：曾逸銘
碩士班研究生-兼任助理人員：蔡欣憲
碩士班研究生-兼任助理人員：張哲瑋
博士班研究生-兼任助理人員：王志哲

報告附件：出席國際會議研究心得報告及發表論文

處理方式：本計畫涉及專利或其他智慧財產權，1年後可公開查詢

中 華 民 國 100 年 10 月 24 日

行政院國家科學委員會專題研究計畫期末報告

多功能微液滴操控平台與陣列式反應器系統的開發

計畫編號：NSC 99-2628-E-007-028

執行期限：99 年 8 月 1 日至 100 年 7 月 31 日

計畫主持人：蘇育全 國立清華大學工程與系統科學系

計畫參與人員：王志哲、張勝智、曾逸銘、蔡欣憲、張哲瑋 國立清華大學工程與系統科學系

中文摘要

本計畫成功開發多功能微液滴操控平台，把耗費大量空間、時間、與人力的化學與生物反應程序，濃縮在一塊佈滿微流道的晶片上自動執行，透過尺度效應與系統整合，大幅提升整體效率並創造全新功能。分散於液態介質中的微液滴擁有良好的空間隔絕特性，具高表面積/體積比能快速傳熱，可容納少量樣本進行快速且多樣化的反應，實現個別反應操控與高度平行處理的目標，使有限樣本發揮最大功效，在最短時間內取得最多資訊以供分析。本計畫透過氣壓驅動軟質彈性薄膜，精確且即時地操控微流道中流體的運動，搭配特殊設計的流道幾何，創造出微液滴產生/定量、融合/混合、多重乳化/結構控制、篩選/置換、暫存/取出、樣本擷取、與檢測等功能。相較於傳統透過驅動壓力/速度控制的做法，彈性薄膜的往復運動可由數位的時序訊號自動控制，透過與電腦軟硬體整合，不僅設計難度降低，系統運作的可靠度和擴充性也有顯著的提昇。以上述功能為基礎，本計畫成功開發適用於生醫檢測與功能材料合成等應用的陣列式反應器系統。個別反應物先形成體積最小可達兆分之一公升的液滴，多重液滴在融合/混合成具特定反應物濃度與比例的單一液滴後開始反應，後續可再：(1)融合/混合液滴以終止或進行多步驟反應，反應時間可精確控制到十分之一秒，(2)執行多步驟乳化程序以形成多重核/多層殼狀結構，或(3)暫存於陣列中長期觀察，依需要取出進行後續處理。此外本計畫也進行細部功能開發、系統軟硬體整合、與效能最佳化等工作，並積極尋求技術與產業發展的新契機。

中文關鍵詞 微液滴、生醫晶片、多重乳化、液滴操控、生醫檢測、微流體系統、微陣列、系統整合

Part I: On-Demand Double Emulsification Utilizing Pneumatically-Actuated, Selectively-Surface-Modified PDMS Micro-Devices

We have successfully demonstrated an active, 2-step emulsification scheme that is capable of producing double emulsions with desired geometries and compositions on demand. PDMS micro-structures with pneumatically actuated membrane-valves constructed on top of specially designed fluidic-channels are utilized to meter and shape immiscible fluids into double emulsions. By varying the timings of membrane actuation, the structures of resulting double-emulsions can be adjusted in a real-time manner. In the prototype demonstration, a three-layer PDMS molding and irreversible bonding process is employed to fabricate the proposed microfluidic devices. It has been demonstrated that (1) the inner and outer diameters can be controlled independently, (2) volume ratios (droplet to drop) ranging from 0.01 to 0.4 can be readily achieved, and (3) adjacent

drops with varying sizes, droplet diameters, and numbers of droplets inside can be produced on demand. As such, the demonstrated emulsification scheme could potentially realize the real-time controllability on emulsion geometries and compositions, which is desired for a variety of applications.

INTRODUCTION

Double emulsions are structured fluids consisting of emulsion drops with smaller droplets inside. Their unique properties and diverse applications have attracted considerable attention to the development of sophisticated production schemes. Traditionally, 2-step emulsification processes, in which the inner fluid is dispersed in the middle fluid first and then the mixture is emulsified in the outer continuous-phase fluid, are employed for the massive production of double emulsions. However, the results are usually ill-controlled in both size and structure, owing to the polydispersity resulting from the processes. The formation of double emulsions is inherently complex and difficult to control. Most existing microfluidic double-emulsification schemes are passive, and controlled mainly by adjusting the flow-rates of the fluids involved [1-4]. They are capable of producing continuous emulsion-streams, while insufficient for adjusting the breakup frequency and emulsion structure in an on-demand manner. To address the desire for real-time controllability on emulsion geometries and compositions, this paper presents an active scheme that can produce and manipulate double emulsions utilizing multilayer microfluidic devices.

OPERATING PRINCIPLE

The active, 2-step emulsification scheme starts with the metering of inner droplets [5]. As illustrated in Figure 1, the collapse of membrane breaks the inner fluid and produces a discrete droplet. Normally, the membrane blocks the dispersed-phase flow completely, while a limited volume of the dispersed-phase fluid can flow through the path when the membrane is up. Subsequently, the droplet is temporally entrapped by the collapse of another membrane downstream, while the middle fluid bypasses the blockage as illustrated in Figure 2. To investigate the relevant flow behavior around the bypassing channel, simulation using ANSYS is performed. Figure 3 shows the simulated velocity distribution when the membrane is either down or up. For droplets with diameters larger than half of the width of the central channel, it is expected that the droplets would be driven into the space between the membrane and the last pair of the bypassing branches, while the continuous-phase fluid bypasses the blockage and keeps flowing downstream. Meanwhile, multiple droplets from parallel sources can be fused here to generate a combined droplet with desired volume and composition. Afterward, the downstream membrane moves up for a certain period of time, during which the droplet and a specific volume of middle fluid pass be-

neath the membrane, and then collapses again. The collapse breaks the middle fluid and produces an emulsion drop with smaller droplets inside.

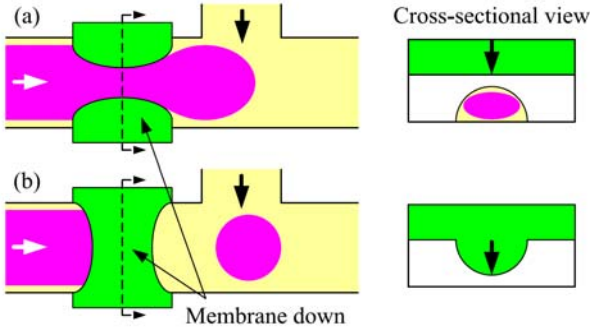


Figure 1: Illustration of the proposed metering scheme.

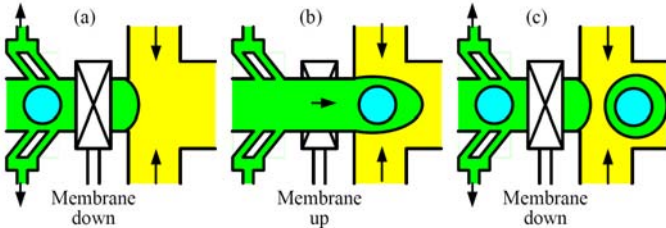


Figure 2: Illustration of the double emulsification scheme.

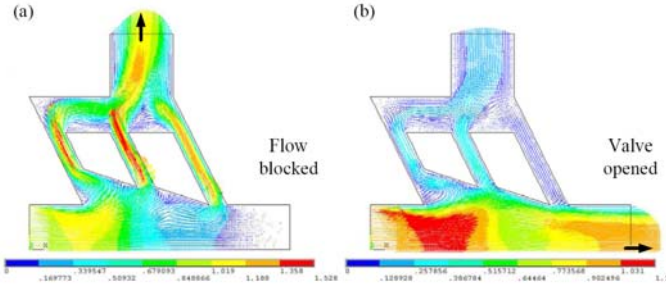


Figure 3: Simulation results of the flow behaviors around a bypassing channel.

FABRICATION PROCESSES

As illustrated in Figure 4, a three-layer molding and bonding process is employed to fabricate the devices, and a fabricated microstructure is shown in Figure 5. First of all, a layer of 25 μm thick positive photoresist (9260, AZ Electronic Materials) is spin-coated and patterned on top of a clean silicon wafer to fabricate the mold used for the duplication of flow-channel layer. Afterward, the patterned photoresist layer is baked at 120 $^{\circ}\text{C}$ for 30 min, during which the photoresist reflows and its profile became rounded. Meanwhile, the mold used for the duplication of control-channel layer is fabricated by coating and patterning a 10 μm thick layer of negative photoresist (SU-8, MicroChem) on top of a clean silicon wafer. After the two photoresist molds are fully cured, they are placed in a desiccator under vacuum for 3 hours with a vial containing a few drops of 1H,1H,2H,2H-perfluorooctyl-trichlorosilane (Fluka) to silanize the surfaces.

A mixture of 10:1 PDMS pre-polymer and curing agent (Sylgard 184, Dow-Corning) is stirred thoroughly and then degassed under vacuum to remove entrapped air bubbles. About 1/3 of the PDMS mixture is poured onto the flow-channel mold, degassed, and cured for 15 minutes at 85 $^{\circ}\text{C}$. Meanwhile, another 1/3 of the PDMS mixture is poured onto

the control-channel mold, degassed, cured for 1 hour at 85 $^{\circ}\text{C}$, and then peeled off from the mold. Afterward, the control-channel layer is pressed and bonded on top of the flow-channel layer, and left undisturbed for at least 1 hour at 85 $^{\circ}\text{C}$ for the bonding to take effect. The bonded, two-layer PDMS structure is then peeled off from the silicon wafer, and punched through with a sharp metal-tube array to fabricate the holes for multiple inlets and outlets. Afterward, it is cleaned in an ultrasonic bath to remove residual debris from its surface. In order to raise the height of flow channel, a second flow-channel layer, which is actually the bottom half of the flow channel, is fabricated using a similar process. The surfaces of the two flow-channel layers are then treated with a hand-held corona treater (BD-20AC, Electro-Technic Products), which ionizes surrounding air and creates localized plasma to activate the surfaces for irreversible bonding. The corona-treated surfaces are then pressed together and left undisturbed for at least 1 hour at 85 $^{\circ}\text{C}$ for the bonding to take effect. At the end, multiple PTFE tubes are inserted into the punched holes to build the necessary interconnection for sample injection and discharge.

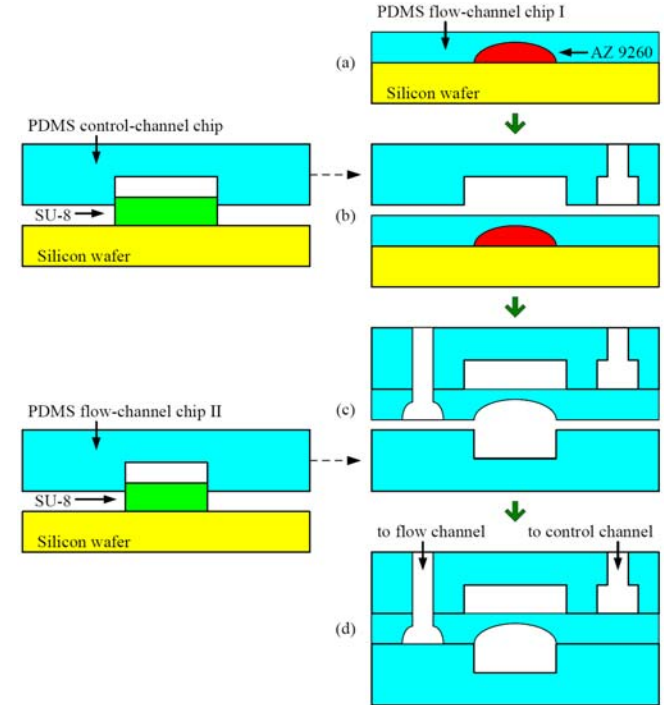


Figure 4: Three-layer PDMS molding and bonding process.

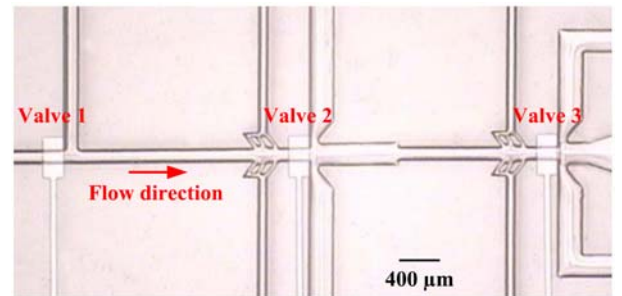


Figure 5: Micrograph of a multiple emulsification device.

EXPERIMENTAL DETAILS

In the prototype demonstration, water-in-oil-in-oil (W/O/O) double emulsions are produced using de-ionized (DI) water, oleic acid (Aldrich) with 5 wt% PGPR 90 (Danisco), and silicone oil (Dow-Corning) as inner, middle, and outer

fluids, respectively. The detailed experimental setup is illustrated in Figure 6. An air compressor (Model 3-4, Jun-Air) with its output set at 500 kPa is employed as the single source to drive the operation. Each fluid sample is stored in a separate plastic container, which is fed with pressurized air from the top to drive the fluid flowing through the bottom tube and into the downstream microfluidic devices. The actual driving pressure applied on each container is adjusted independently by a separate pressure regulator (IR1000-01G, SMC). Meanwhile, the actuation of each membrane valve is controlled independently by a separate electromagnetic valve (VK332-5G-M5, SMC), whose action is governed by a computer-controlled relay circuitry. A governing program developed and executed under a software environment (LabVIEW, National Instruments), cooperating with a set of hardware adapter and connector (PCI-6220 + CB-68LP), is employed to coordinate the actuation of the prototype system. As such, the operation can be either preprogrammed or responding to demand in a real-time manner.

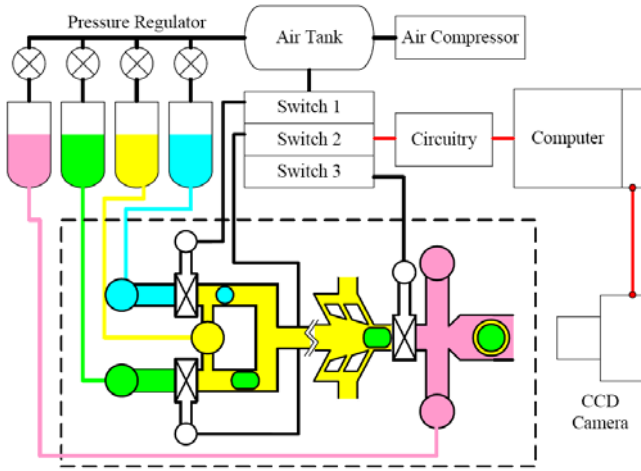


Figure 6: Experimental setup of the emulsification scheme.

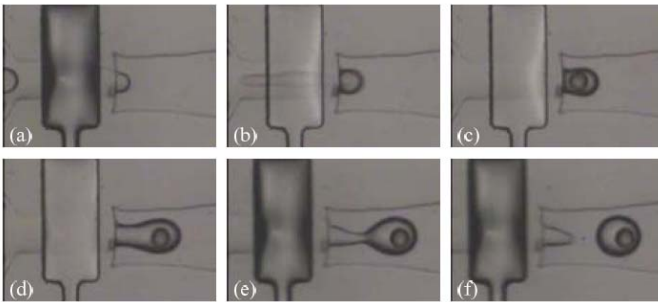


Figure 7: Captured two-step double emulsification sequence.

RESULTS AND DISCUSSION

Double emulsification is successfully demonstrated using the devices, and a captured sequence is shown in Figure 7. A water droplet is metered using the first membrane valve, and temporally entrapped in front of the second one. Afterward, the second membrane moves up for a certain period of time, during which the droplet and a specific volume of middle fluid pass beneath the membrane, and then collapses again. Figure 8 shows the measured relationship between resulting drop sizes and the open time of second membrane valve. It is found that the overall drop volume is proportional to the valve-open time, while affected insignificantly by the volume of inner droplets. In this 2-step emulsification scheme, the overall and droplet volumes can be adjusted

readily and independently. As shown in Figure 9, the front of a larger entrapped droplet is deeper into the dead volume, and therefore it is expected that the corresponding droplet-to-drop volume ratio will also be higher (if the valve-open time keeps the same). Figure 10 shows the measured relationship between droplet-to-drop volume ratio and droplet volume. The maximal volume ratio currently we can achieve is less than 40%, which corresponds to a diameter ratio of roughly 74%. Meanwhile, multiple droplets can be metered and encapsulated in a single drop as well. Finally, the formation of adjacent drops with varying sizes, droplet diameters, and numbers of droplets inside is successfully demonstrated as shown in Figure 11. Coordinated by a set of programs and hardware, the timings of membrane actuation can be controlled automatically, either preprogrammed or responding to demand in a real-time manner. The demonstrated devices can only generate W/O/O double emulsions. We are working on the modification and patterning of PDMS surfaces, try to generate patterns capable of facilitating the formation of W/O/W double emulsions.

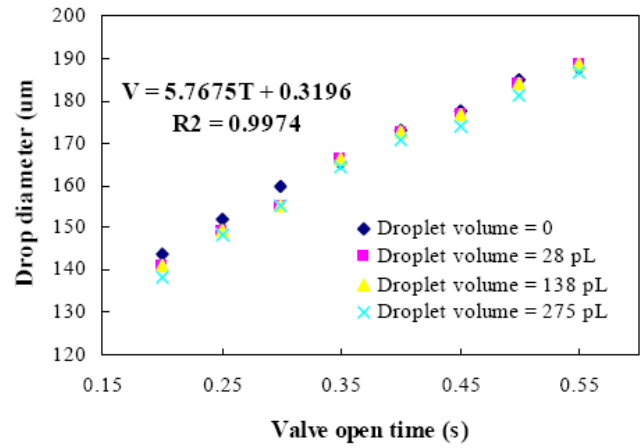


Figure 8: Measured relationship between valve open time and emulsion sizes.

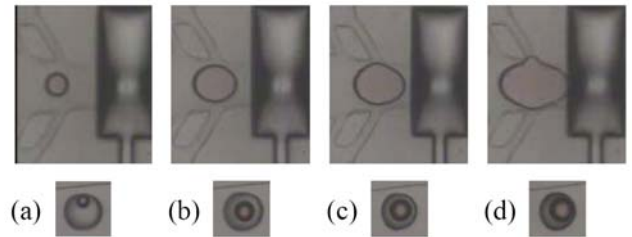


Figure 9: Size-dependent droplet entrainment (upper) and the resulting variation in emulsion structure (lower).

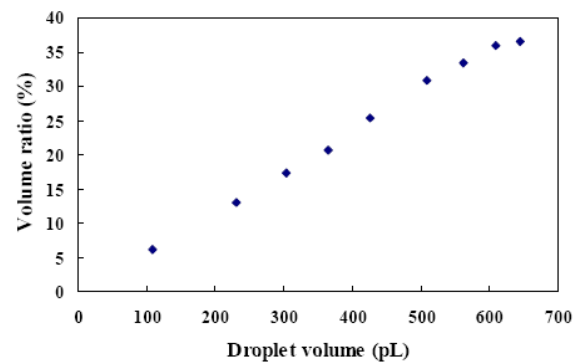


Figure 10: Measured relationship between entrapped droplet volume and droplet/drop volume ratio.

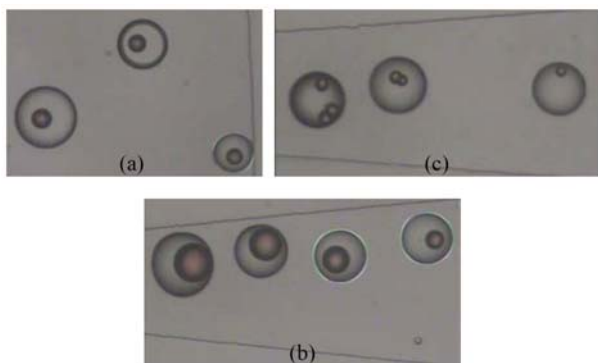


Figure 11: Resulting adjacent drops with varying (a) overall sizes, (b) droplet sizes, and (c) numbers of droplets.

CONCLUSION

This paper presents an active, 2-step emulsification scheme that is capable of producing double emulsions with desired geometries and compositions on demand. PDMS microstructures with pneumatically actuated membrane-valves constructed on top of specially designed fluidic-channels are utilized to meter and shape immiscible fluids into double emulsions. By varying the timings of membrane actuation, the structures of resulting double-emulsions can be adjusted in a real-time manner. In the prototype demonstration, a three-layer PDMS molding and irreversible bonding process is employed to fabricate the proposed microfluidic devices. It has been demonstrated that (1) the inner and outer diameters can be controlled independently, (2) volume ratios (droplet to drop) ranging from 0.01 to 0.4 can be readily achieved, and (3) adjacent drops with varying sizes, droplet diameters, and numbers of droplets inside can be produced on demand. Currently the demonstrated devices can only generate W/O/O double emulsions. We are working on the modification and patterning of PDMS surfaces, and trying to generate patterns capable of facilitating the formation of W/O/W double emulsions. As such, the proposed emulsification scheme could potentially realize the real-time controllability on emulsion geometries and compositions, which is desired for a variety of applications.

REFERENCES

- [1] S. Okushima, T. Nisisako, T. Torii and T. Higuchi, "Controlled Production of Monodisperse Double Emulsions by Two-Step Droplet Breakup in Microfluidic Devices," *Langmuir*, 20, pp. 9905–8, 2004.
- [2] A.S. Utada, E. Lorenceau, D.R. Link, P.D. Kaplan, H. A. Stone and D.A. Weitz, "Monodisperse Double Emulsions Generated from a Microcapillary Device," *Science*, 308, pp. 537–41, 2005.
- [3] M. Seo, C. Paquet, Z. Nie, S. Xu and E. Kumacheva, "Microfluidic Consecutive Flow-Focusing Droplet Generators," *Soft Matter*, 3, pp. 986–92, 2007.
- [4] F.-C. Chang and Y.-C. Su, "Controlled Double Emulsification Utilizing 3D PDMS Microchannels," *J. Micromechanics and Microengineering*, 18, #065018, 2008.
- [5] B.-C. Lin and Y.-C. Su, "On-Demand Liquid-in-Liquid Droplet Metering and Fusion Utilizing Pneumatically-Actuated Membrane Valves," *J. Micromechanics and Microengineering*, 18, #115005, 2008.

Part II: A Random-Access Droplet Storage Array for Programmable Reaction Screening

This paper presents a microfluidic array that is capable of randomly storing and discharging droplets on demand. A microdevice with multilayer fluidic channels dynamically reconfigured by diaphragm valves is used to realize the random access process. In the prototype demonstration, droplets with desired geometries and compositions are generated, selectively stored, and discharged from a 4×4 array, which employs just 4 ($=2 \times \log_2 4$) control inputs for the operation. With droplets functioning as micro-reactors, the proposed random-access storage array could potentially serve as a platform for parallel and multi-step reaction control, which is desired for high-throughput screening applications.

INTRODUCTION

Among the various types of high-throughput, microfluidic screening systems, droplet-based systems have recently attracted significant interest because of their potential impacts on diverse chemical and biological applications [1-2]. By compartmentalizing reactions into tiny droplets, the miniaturization and parallel processing of reactions, which are desired for applications involving the investigation of huge parameter spaces, could eventually be realized. The resulting low sample consumption and high reaction throughput are expected to significantly accelerate the progress in drug discovery, protein crystallization, and various chemical and biological screening and synthesis. To address the need for controllability on parallel and multi-step reactions, this paper presents a PDMS micro-array that is capable of randomly storing and discharging droplets on demand. Three accomplishments have been achieved: (1) a bi-directional diaphragm valve, (2) a pneumatic inverter, and (3) a random-access droplet storage array utilizing minimum control inputs. As such, droplet reactors could be temporarily stored, re-injected, monitored, or discharged for further processing, all in desired and programmable manners.

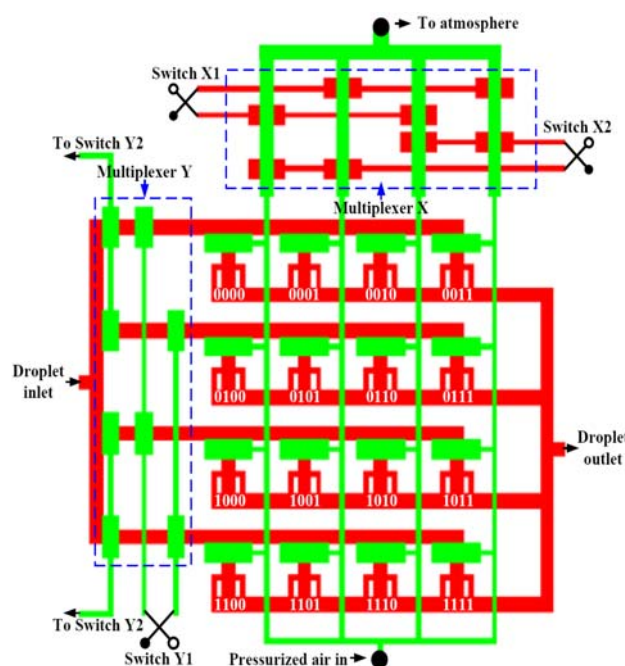


Figure 1: Schematic illustration of the storage array

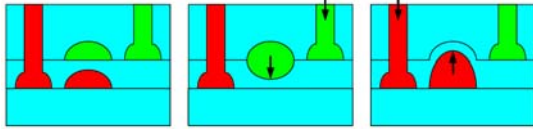


Figure 2: Cross-sectional view of the storage array

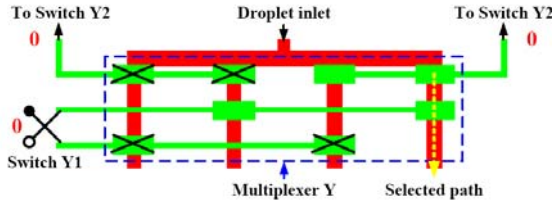


Figure 3: Schematic illustration of Multiplexer Y

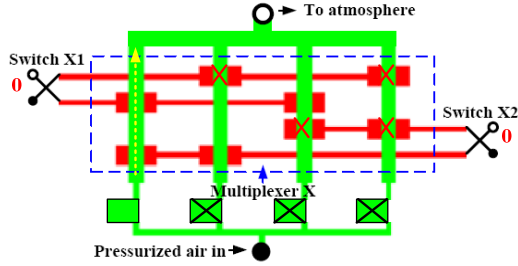


Figure 4: Schematic illustration of Multiplexer X

OPERATING PRINCIPLE

A schematic illustration of the proposed 4×4 droplet storage array is shown in Figure 1. Multiplexer X and Y are employed to control the flow path and therefore the destination of an incoming or temporarily stored droplet. An incoming droplet in the bottom fluid channel will first arrive at the inlet, and then be directed to one of the four flow paths by Multiplexer Y. Once into the selected flow path, the droplet will be driven further into one of the four storage units determined by Multiplexer X. A cross-sectional view of the three-layered storage array is illustrated in Figure 2. An elastic PDMS diaphragm is constructed between two layers of fluidic channels, so either channel could be pressurized to block the flow in the other channel. It functions as a bi-directional diaphragm valve, which could greatly simplify the integration of multiple pneumatic logic components on one single microfluidic chip. For multiplexer Y (as illustrated in Figure 3), pressurized air is filled into the top fluidic channel, so the diaphragm move downwards to block the underneath liquid flow in 3 out of 4 flow paths. For multiplexer X (as illustrated in Figure 4), pressurized air is filled into the bottom fluidic channel, so 3 out of 4 flow paths in the top fluidic channel are blocked, which leads to pressurization of these flow paths. In addition, the pressurization also causes the diaphragm along these flow paths to move downwards, which results in the blockage in 3 out of the four columns. Therefore, the droplet will be driven into the only column which fluid is allowed to pass through. As such, a pneumatic inverter is realized utilizing the bi-directional diaphragm valve. Overall 4 control inputs (Y2Y1X2X1) are employed to operate the 4×4 array, and the corresponding destinations of all input combination are labeled in Figure 1. For an $M \times M$ array, only $2 \times \log_2 M$ control inputs are required for its operation. Once the droplet arrives at the desired storage unit, the flow path is blocked to stop and entrap the droplet. At the end, a trapped droplet could be discharged from a storage unit simply by

re-directing the flow to pass through the storage unit, so the droplet will be dragged along the flow path and finally to the outlet.

EXPERIMENTAL

The fabrication of the proposed droplet storage array is illustrated Figure 5. First of all, a layer of $25 \mu\text{m}$ thick positive photoresist (9260, AZ Electronic Materials) is spin-coated and patterned on top of a clean silicon wafer to fabricate the mold used for the duplication of bottom flow-channel layer. Afterward, the patterned photoresist layer is baked at 120°C for 30 min, during which the photoresist reflows and its profile became rounded. Meanwhile, the mold used for top flow-channel layer is fabricated using the same process. After the two photoresist molds are fully cured, they are placed in a desiccator under vacuum for 3 hours with a vial containing a few drops of 1H,1H,2H,2H-perfluorooctyl-trichlorosilane (Fluka) to silanize the surfaces. A mixture of 10:1 PDMS pre-polymer and curing agent (Sylgard 184, Dow-Corning) is stirred thoroughly and then degassed under vacuum to remove entrapped air bubbles. Less than $1/5$ of the PDMS mixture is poured onto the bottom flow-channel mold, degassed, and cured for 15 minutes at 85°C . Meanwhile, another $2/5$ of the PDMS mixture is poured onto the top flow-channel mold, degassed, cured for 1 hour at 85°C , and then peeled off from the mold. Afterward, the top flow-channel layer is pressed and bonded on top of the bottom flow-channel layer, and left undisturbed for at least 1 hour at 85°C for the bonding to take effect. The bonded, two-layer PDMS structure is then peeled off from the silicon wafer, and punched through with a sharp metal-tube array to fabricate the holes for multiple inlets and outlets. Afterward, it is cleaned in an ultrasonic bath to remove residual debris from its surface, and finally corona-treated and bonded irreversibly on a blank PDMS substrate. At the end, multiple PTFE tubes are inserted into the punched holes to build the necessary interconnection. A governing program developed and executed under a software environment (LabVIEW, National Instruments), cooperating with a set of hardware adapter and connector (PCI-6220 + CB-68LP), is employed to coordinate the actuation of the prototype system. As such, the operation could be either preprogrammed or responding to demand in a real-time manner.

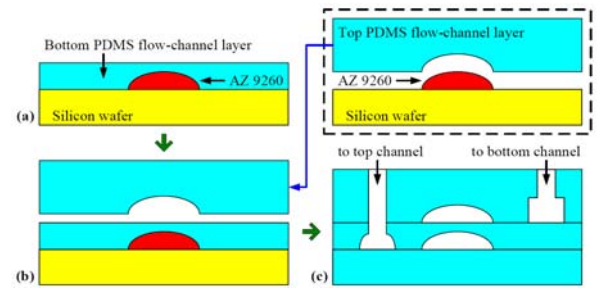


Figure 5: Fabrication of the droplet storage array

RESULTS AND DISCUSSION

In the prototype demonstration, droplets with desired geometries and compositions are generated [3, 4] and fed into the storage array. With the integration of an additional diaphragm valve (back door) into the storage unit, as illustrated in Figure 6, a droplet could be securely trapped even when the upstream valve (front door) is opened. As also

illustrated in Figure 6, re-injection of materials into a droplet reactor could be realized by the controlled coalescence of droplets. The opening of the front door will bring the flow and therefore the coming droplet in, while the closing of the back door will entrap the droplet but not block the flow. The flow bypasses the blockage turning up- and downwards. All the back door valves are governed by one extra control input. When these valves are closed and opened, the array is ready for droplet storing/re-injection and discharging, respectively. Figure 7 illustrates a recorded random storing and discharging sequence. Droplets are dragged from left to right, and stored following the 1 to 8 order labeled on the figure. It is noticed that all diaphragm valves switch smoothly, and droplets move into assigned storage units just as planned. Meanwhile, it is also demonstrated that the stored droplets could be discharged in an arbitrary order. For example, droplet discharging in an order of 5-6-7-8-1-2-3-4 is illustrated in Figure 7. As such, droplet reactors could be temporarily stored, re-injected, monitored, or discharged for further processing, all in desired and programmable manners. In addition to the three-layered process, we have further developed a four-layered fabrication process. A flow-channel is sandwiched by upper and lower control-channels, whose pressurization would cause the diaphragms to collapse down- and upwards, respectively, and block the flow-channel. With the addition of one more structure layer, the design and integration of pneumatic logic components and systems could be greatly simplified. We are currently working on the integration of sorting and oscillation functions into the system and trying to reduce the overall volume at the same time. As such, this droplet storage array could potentially serve as a platform for parallel, multi-function, and multi-step reaction control, which is desired for high-throughput screening applications.

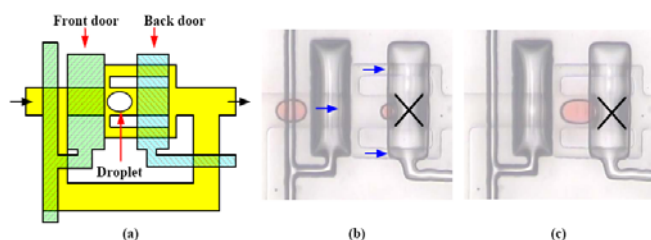


Figure 6: Illustration of a storage unit with two valves

CONCLUSION

We have successfully demonstrated a microfluidic array that is capable of randomly storing and discharging droplets on demand. A PDMS microdevice with multilayer fluidic-channels dynamically re-configured by diaphragm valves is utilized to realize the random-access process. In the prototype demonstration, droplets with desired geometries and compositions are generated, selectively stored, and discharged from a 4×4 array, which employs just 4 ($=2 \times \log_2 4$) control inputs for the operation. With droplets functioning as micro-reactors, the proposed random-access storage array could potentially serve as a platform for parallel, multi-function, and multi-step reaction control, which is desired for high-throughput screening applications.

REFERENCES

- [1] Song H, Chen D, and Ismagilov R 2006 Reactions in droplets in microfluidic channels *ANGEW CHEM INT EDIT* **45** 7336
- [2] Kelly B, Baret J, Taly V, and Griffiths D 2007 Miniaturizing chemistry and biology in microdroplets *CHEM COMMUN* **18** 1773
- [3] Lin B and Su Y 2008 On-demand liquid-in-liquid droplet metering and fusion utilizing pneumatically actuated membrane valves *J MICROMECH MICROENG* **18** #115005
- [4] Lin H, Chang S, and Su Y 2010 On-demand double emulsification utilizing pneumatically actuated, selectively surface-modified PDMS micro-devices *MICROFLUID NANOFUID*, Published online

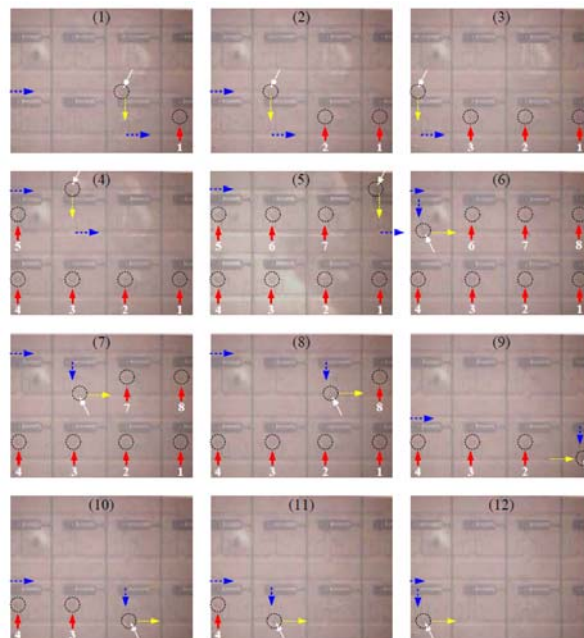


Figure 7: A captured sequence of random storing and discharging utilizing the droplet storage array

PART III: On-Demand Micro Encapsulation Utilizing On-Chip Synthesis of Semi-Permeable Alginate-PLL Capsules

This paper presents an on-demand, multi-step synthesis scheme that is capable of forming semi-permeable microcapsules on an integrated microfluidic chip. Three-layered PDMS devices with pneumatically actuated diaphragm-valves constructed on specially designed fluidic-channels are utilized to realize the encapsulation process. In the prototype demonstration, Na-alginate droplets are metered, trapped, and then drawn into CaCl_2 droplets, while they react and form solid Ca-alginate microcapsules on the interfaces. In addition, entrapment and transfer of the resulting capsules can also be performed on the same microfluidic chip to further process Ca-alginate into semipermeable alginate-PLL. As such, the demonstrated on-chip synthesis scheme could potentially fulfill the real-time controllability on micro-encapsulation, which is desired for a variety of biological and medical applications.

INTRODUCTION

Because of the strong application potential, considerable attention has been attracted to the development of controllable and reliable double emulsification schemes. Recently, researchers have demonstrated double emulsification in

various microfluidic devices utilizing two-step breakup [1] and 3D flow focusing [2]. In addition, it has also been demonstrated that the middle liquid in a double emulsion can be further processed into a solid capsule [3]. For example, polymeric materials can be dissolved in the middle organic solvent, and solidified into microcapsules once the solvent is extracted. Meanwhile, microcapsules can also be fabricated by forming emulsion droplets with microfluidic devices first, and then collecting and transferring them into specific medium for sequential reactions on the droplet interfaces [4]. Most microfluidic emulsification utilizing passive schemes, which are capable of producing continuous droplet streams, but insufficient for adjusting droplet size and manipulating droplet movement in a real-time manner [5]. For multi-step processes such as encapsulation and sequential surface modification, off-chip operation is usually required. To address the need for real-time controllability on micro-encapsulation, this paper presents an integrated microfluidic system that could form semi-permeable micro-capsules with desired geometries and compositions on demand. Emulsion droplets functioning as templates and reactors are employed to realize the synthesis process. Devices with pneumatically actuated diaphragm-valves constructed on specially designed fluidic-channels are utilized to control the droplets, and consequently the encapsulation process. Three accomplishments have been achieved: (1) a diaphragm-actuated emulsification and entrapment device that can produce monodisperse droplets with desired sizes, and selectively entrap droplets and solid capsules in a real-time manner; (2) a multi-step reaction scheme can be performed on droplet-in-droplet interfaces to synthesize alginate-poly-L-lysine (PLL) capsules; and (3) an active, integrated microfluidic system that can produce semi-permeable microcapsules with desired sizes and compositions on demand. Superior to the previously reported double emulsification and multi-step synthesis schemes, the demonstrated microfluidic devices could potentially fulfill the real-time controllability on encapsulation, which is desired for a variety of applications.

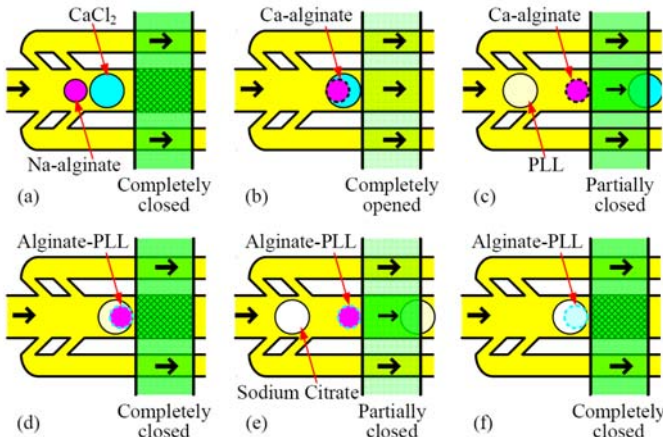
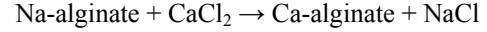


Figure 1: Schematic of the proposed encapsulation scheme

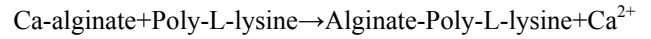
OPERATING PRINCIPLE

A schematic illustration of the proposed micro encapsulation scheme is shown in Figure 1. A three-layered microfluidic chip with pneumatically actuated diaphragm valves built on specially designed microfluidic channels is utilized to perform the multi-step synthesis process. The complete collapse of a diaphragm on the central flow-path stops the

droplets and results in the merger into a double-emulsion structure (Figure 1-a). Two droplets containing aqueous Na-alginate and CaCl_2 solutions individually react on the interface to form a solid Ca-alginate capsule (Figure 1-b) as the following:



The diaphragm-valve is then partially opened, which allows outer un-reacted CaCl_2 solution to pass while the solid capsule remains trapped (Figure 1-c). The trapped capsule is rinsed by an incoming buffer droplet and then re-suspended into another incoming droplet containing PLL, while the valve turns completely closed (Figure 1-d). Re-suspension of the capsules into PLL solution results in the formation of an alginate-PLL capsule due to the poly- ion complex:



Once an alginate-PLL capsule is formed, it is rinsed and then re-suspended into a droplet of sodium-citrate solution to dissolve unreacted Ca-alginate gel inside the capsule (Figure 1-e). At the end, an alginate-PLL capsule is formed with its core in liquid state, and released for sequential processing (Figure 1-f). Meanwhile, a T-junction with a diaphragm valve mounted on its top (as shown in Figure 2) is employed to control the metering process [6].

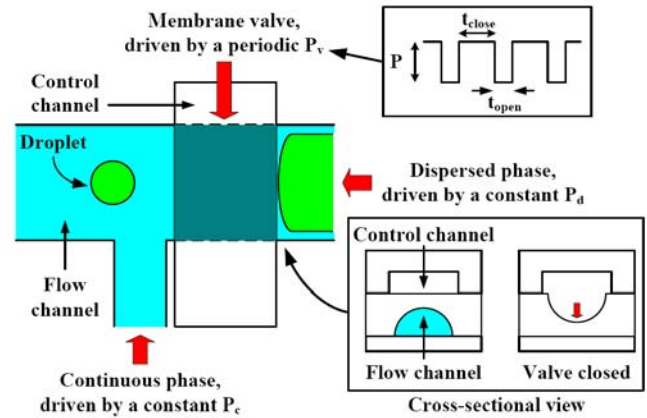


Figure 2: Schematic of the proposed metering scheme

FABRICATION PROCESSES

A 3-layered, PDMS molding and irreversible bonding process was employed to fabricate the proposed microfluidic chip, as illustrated in Figure 3. First of all, a layer of 25 μm thick positive photoresist (9260, AZ Electronic Materials) was spin-coated and patterned on top of a clean silicon wafer to fabricate the mold used for duplicating the top half of the flow channel. Afterwards, the patterned photoresist layer was baked at 120 $^\circ\text{C}$ for 30 min, during which the photoresist reflowed and its profile became rounded. Meanwhile, the molds used for duplicating the control channel and the bottom half of flow channel were fabricated by coating and patterning 10 μm and 100 μm thick layers of negative photoresist (SU-8, MicroChem) on top of clean silicon wafers, respectively. After the three photoresist molds were fully cured, they were placed in a desiccator under vacuum for 3 hours with a vial containing a few drops of 1H,1H,2H,2H-per-fluorooctyl-trichlorosilane (Fluka) to silanize the surfaces. A mixture of 10:1 PDMS pre-polymer and curing

agent (Sylgard 184, Dow-Corning) was stirred thoroughly and then degassed under vacuum to remove entrapped air bubbles. The casting and bonding process started with the deposition of a thin PDMS mixture layer on top of the top flow-channel mold. About one tenth of the PDMS mixture was spin-coated on the mold at 2000 rpm for 30 seconds, which yielded a thickness of roughly 50 μm , and cured for 15 minutes at 85°C. Meanwhile, about half of the PDMS mixture was poured onto the control-channel mold, degassed, cured for 15 minutes at 85°C, and then peeled off from the mold. Afterwards, the control-channel layer was pressed and bonded on top of the 50 μm -thick top flow-channel layer, and left undisturbed for at least 1 hour at 85°C for the bonding to take effect. The bonded, two-layer PDMS structure was then peeled off from the silicon wafer, and punched through with a sharp metal-tube array to fabricate the holes for multiple inlets and outlets. Meanwhile, the left PDMS mixture was poured onto the bottom flow-channel mold, degassed, cured for 1 hour at 85°C, and then peeled off from the mold. The surfaces of the two-layer PDMS structure (on the flow channel side) and the duplicated bottom flow-channel layer were then treated with a hand-held corona treater (BD-20AC, Electro-Technic Products), which ionizes surrounding air and creates localized plasma to activate the surfaces for irreversible bonding. The corona-treated surfaces were then pressed together and left undisturbed for at least 1 hour at 85°C for the bonding to take effect. At the end, multiple PTFE tubes were inserted into the punched holes to build the necessary interconnection for compressed air supply and fluidic sample injection and discharge.

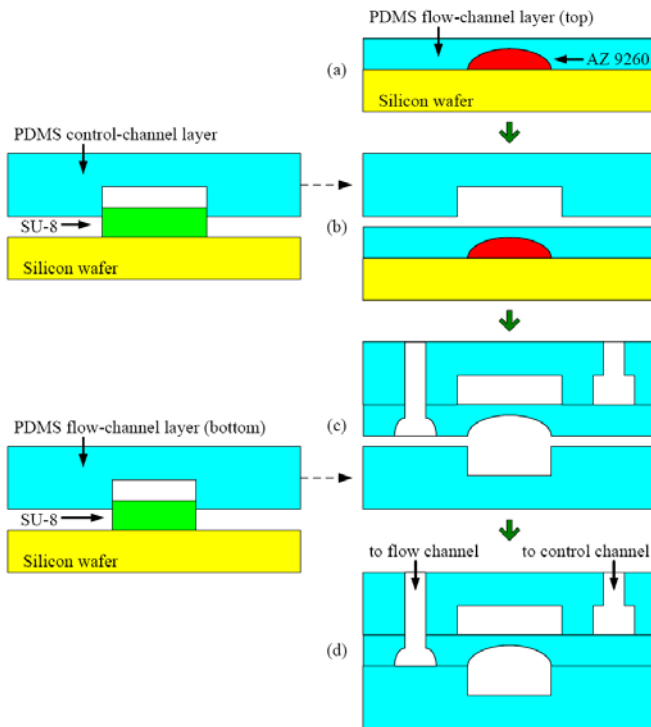


Figure 3: A 3-layered, PDMS molding and bonding process

EXPERIMENTAL DETAILS

The operation of the presented integrated system is illustrated in Figure 4. An air compressor (Model 3-4, Jun-Air) with its output set at 500 kPa was employed as the single pressure source to drive the operation. Each liquid sample was stored in a separate plastic container, which was

fed with pressurized air from the top to drive the sample flowing through the bottom tube and into the downstream microfluidic devices. The actual driving pressure applied on each container was adjusted independently by a separate pressure regulator (IR1000-01G, SMC). Meanwhile, the actuation of each diaphragm valve was controlled independently by a separate electromagnetic valve (VK332-5G-M5, SMC), whose action was governed by a computer controlled relay circuitry. A governing program developed and executed under a software environment (LabVIEW, National Instruments), cooperating with a set of hardware adapter and connector (PCI-6220 + CB-68LP), was employed to coordinate the actuation of the prototype system. As such, the operation can be either pre-programmed or responding to demand in a real-time manner. The emulsification and encapsulation processes were observed under an optical microscope and the images were recorded using either a standard CCD camera (SSC-DC80, SONY) or a high-speed digital camera (SR series, KODAK Motion Corder Analyzer), which was also connected to the computer. The resulting droplets and capsules were driven into a 200 μm deep reservoir, where droplets and capsules would be perfect spheres without unwanted deformation. The volumes of the droplets and capsules were estimated based on the observed spherical diameters.

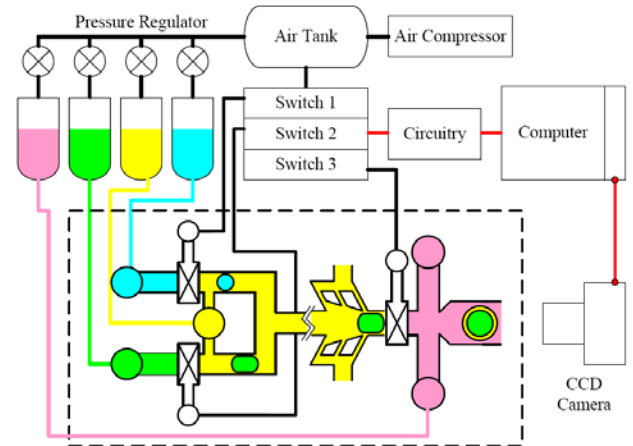


Figure 4: Experimental setup of the encapsulation scheme

RESULTS AND DISCUSSION

The injection of a relatively small Na-alginate droplet into a relatively large CaCl_2 droplet is the most critical step in the proposed encapsulation process. Figure 5 shows images of two injection sequences with Na-alginate droplets of 150 and 100 μm in diameter. Concentration (and consequently the viscosity) of the left-hand side Na-alginate droplet is found to dramatically affect the shape of the resulting Ca-alginate capsule. With a Na-alginate concentration of 1 wt%, the shapes of the resulting Ca-alginate capsules, as shown in Figure 5, are sickle like. Since the viscosities of Na-alginate and calcium chloride solutions are around the same order, in these cases the Na-alginate droplets are greatly deformed by the flow inside the calcium chloride droplets. In around 10 (Figure 5-a) and 5 (Figure 5-b) milliseconds, the interfaces between Na-alginate and calcium chloride droplets solidify and Ca-alginate capsules are formed. However, the application of these capsules would be limited because of their sickle like shapes. Fortunately, it is also found that with a concentration higher than 3 wt%, the viscosity of a Na-alginate solution becomes much higher than that of a calcium chloride solution with a concentration remaining at

1.5 wt%. When a highly viscous Na-alginate droplet is drawn into a dilute calcium chloride droplet (as illustrated later in Figure 6), it remains intact and solidifies to form a circular-shaped Ca-alginate capsule.

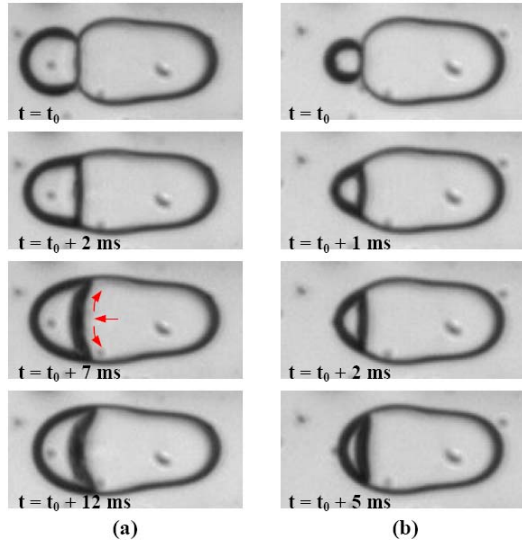


Figure 5: Captured sequences of droplet coalesce with droplet diameters of 150 μm (a) and 100 μm (b)

Controlled encapsulation was successfully demonstrated using the fabricated microfluidic devices, and a captured encapsulation sequence is shown in Figure 6. First of all, Na-alginate and CaCl_2 droplets are metered and selectively trapped in front of a collapsed diaphragm, whose movement further results in the merger of droplets into a double-emulsion structure. The retreat of the diaphragm (Figure 6-b~c) causes a negative pressure gradient, which sucks in the liquids and in turn accelerates the draining of the liquid film between the trapped droplets. Meanwhile, the re-collapse of the diaphragm (Figure 6-e~f) remains the double-emulsion structure trapped in front of the diaphragm. In the demonstration, overall three solid Ca-alginate capsules are formed in a CaCl_2 droplet (Figure 6-g) using the same approach. Afterwards, the diaphragm valve is partially opened. The solid capsules remain trapped (Figure 6-h~i), while un-reacted CaCl_2 solution is dragged away by the continuous-phase flow. The partial collapse of the diaphragm, which can be adjusted by the applying pressure, is estimated to leave a gap of about 50 μm in width and 10 μm in height. Once un-reacted solution is largely dragged away, the solid capsules are pushed back by the complete collapse of the diaphragm (Figure 6-j). Furthermore, rinse and re-suspension of the solid capsules are also demonstrated by the coalescence with droplets of buffer and PLL solutions, respectively. Finally, re-suspension of the Ca-alginate capsules into a PLL-solution droplet results in the formation of alginate-PLL capsules (Figure 6-k~l). Once alginate-PLL capsules are formed, they are rinsed and then re-suspended into a droplet of sodium-citrate solution to dissolve unreacted Ca-alginate gel inside the capsule. The semi-permeability and flexibility of the resulting liquid cored alginate-PLL capsules is tested by re-suspending the capsules into a droplet with a relatively low osmotic pressure. To facilitate the observation on capsule deformation, particles of 5 μm in diameter are dispersed in Na-alginate droplets at the beginning and eventually deposited on the surfaces of the capsules. It is observed that the capsule

expands and therefore the distance between two specific deposited particles increases over time. The capsule becomes more transparent while it expands. Meanwhile, the capsule shrinks in case it is re-suspended into a droplet with a relatively high osmotic pressure. The expansion and shrinkage can be reversed and repeated if the droplet is re-suspended into corresponding droplets. In addition, an alginate-PLL capsule with liquid core can be contracted or stretched when forces applying on it.

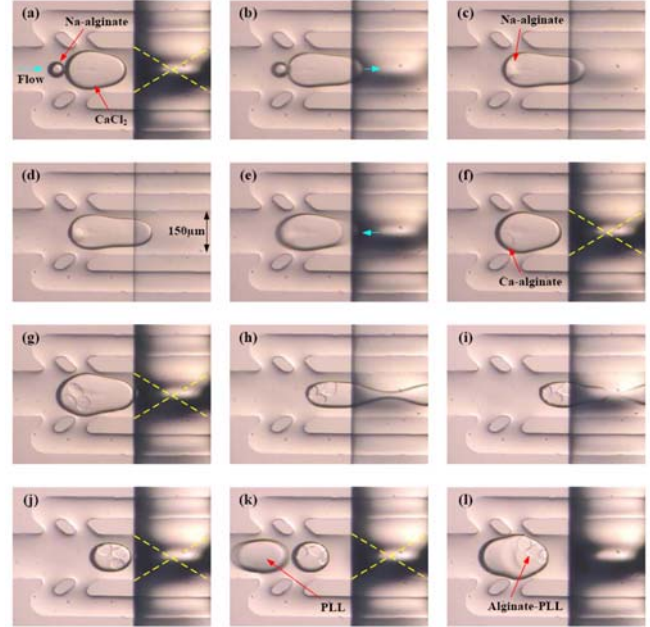


Figure 6: A captured controlled encapsulation sequence

CONCLUSION

We have successfully demonstrated an on-demand, multi-step synthesis scheme that is capable of forming semi-permeable micro-capsules on an integrated microfluidic chip. Emulsion droplets functioning as templates and reactors are employed to realize the multi-step synthesis process. Three-layered PDMS micro-devices with diaphragm-valves constructed on specially designed fluidic-channels are utilized to control the droplets, and consequently the encapsulation process. In the prototype demonstration, a governing computer program cooperating with a set of control hardware was employed to coordinate the actuation of the system. Relatively small Na-alginate droplets are metered, trapped, and then injected into relatively large CaCl_2 droplets, while they react and form solid Ca-alginate micro-capsules on the interfaces. In addition, entrapment and transfer of the resulting capsules can also be performed on the same microfluidic system to further react Ca-alginate into semi-permeable alginate-PLL. It has been demonstrated that: (1) both emulsion droplets and solid capsules could be manipulated; (2) multi-step reactions could be performed on droplet-in-droplet interfaces to synthesize alginate-PLL capsules; and (3) on demand, controlled encapsulation could be achieved on one single microfluidic system.

REFERENCES

- [1] S. Okushima, T. Nisisako, T. Torii, and T. Higuchi, "Controlled production of monodisperse double emulsions by two-step droplet breakup in microfluidic devices", *LANGMUIR* **20**, 9905–8, 2004
- [2] A. Utada, E. Lorenceau, D. Link, P. Kaplan, H. Stone,

- and D. Weitz, "Monodisperse double emulsions generated from a microcapillary device", *SCIENCE* **308**, 537-41, 2005
- [3] C. Liao and Y. Su, "Formation of biodegradable microcapsules utilizing 3D, selectively surface modified PDMS microfluidic devices", *BIOMED MICRO-DEVICES* **12**, 125-33, 2010
- [4] Y. Morimoto, W. Tan, Y. Tsuda, and S. Takeuchi, "Monodisperse semi-permeable microcapsules for continuous observation of cells", *LAB CHIP* **9**, 2217-23, 2009
- [5] M. Joanicot and A. Ajdari, "Droplet control for microfluidics", *SCIENCE* **309**, 887-8, 2005
- [6] B. Lin and Y. Su, "On-demand liquid-in-liquid droplet metering and fusion utilizing pneumatically-actuated membrane valves", *J MICROMECH MICROENG* **18**, #115005, 2008

計畫成果自評

本計畫成功開發多功能微液滴操控平台，把耗費大量空間、時間、與人力的化學與生物反應程序，濃縮在一塊佈滿微流道的晶片上自動執行，透過尺度效應與系統整合，大幅提升整體效率並創造全新功能。分散於液態介質中的微液滴擁有良好的空間隔絕特性，具高表面積/體積比能快速傳熱，可容納少量樣本進行快速且多樣化的反應，實現個別反應操控與高度平行處理的目標，使有限樣本發揮最大功效，在最短時間內取得最多資訊以供分析。本計畫透過氣壓驅動軟質彈性薄膜，精確且即時地操控微流道中流體的運動，搭配特殊設計的流道幾何，創造出微液滴產生/定量、融合/混合、多重乳化/結構控制、篩選/置換、暫存/取出、樣本擷取、與檢測等功能。相較於傳統透過驅動壓力/速度控制的做法，彈性薄膜的往復運動可由數位的時序訊號自動控制，透過與電腦軟硬體整合，不僅設計難度降低，系統運作的可靠度和擴充性也有顯著的提昇。以上述功能為基礎，本計畫成功開發適用於生醫檢測與功能材料合成等應用的陣列式反應器系統。個別反應物先形成體積最小可達兆分之一公升的液滴，多重液滴在融合/混合成具特定反應物濃度與比例的單一液滴後開始反應，後續可再：(1)融合/混合液滴以終止或進行多步驟反應，反應時間可精確控制到十分之一秒，(2)執行多步驟乳化程序以形成多重核/多層殼狀結構，或(3)暫存於陣列中長期觀察，依需要取出進行後續處理。此外本計畫也進行細部功能開發、系統軟硬體整合、與效能最佳化等工作，並積極尋求技術與產業發展的新契機。

快速樣本製備與反應條件篩選技術的發展將會為生化檢驗相關研究帶來多方面的衝擊。以本計畫主要的應用領域，奈米粒子與觸媒合成、蛋白質晶體成長與分析、藥物與細胞/微生物包埋、以及生醫檢測等應用而言，在生活上生醫檢測所需的時間可以被縮短，檢查的項目可以增加，在產業上材料或藥物的開發週期將可以被有效的縮減，成本可以大幅降低，並且迅速的累積在藥物設計與測試等各方面的經驗。在學術上，新技術將可以取代目前一般實驗室中所使用，以人工處理樣本，既緩慢又會消耗大量載具與樣本的實驗程序，有效的加速實驗流程、降低成本、擴展研究範圍，並且提升實驗的整體效能。初步成果已經發表在三篇碩士學位論文，四篇國際研討會論文(MicroTAS and Transducers)，以及三篇SCI

期刊論文(Nanofluidics and Microfluidics and JMM)。透過逐步建立的基礎，投入人力進行深入研究，陸續將有更多更有價值的成果可以被發表於期刊與國際會議。

國科會補助專題研究計畫項下出席國際學術會議心得報告

日期：100 年 6 月 10 日

計畫編號	NSC99-2628-E-007-028-		
計畫名稱	多功能微液滴操控平台與陣列式反應器系統的開發		
出國人員 姓名	蘇育全	服務機構 及職稱	國立清華大學工程與系統科學系
會議時間	100 年 6 月 5 日至 100 年 6 月 9 日	會議地點	中國北京
會議名稱	第十六屆固態感測、致動與微系統國際學術研討會 16th International Conference on Solid-State Sensors, Actuators and Microsystems		
發表論文 題目	1. 多步驟藻酸鹽-聚離胺酸半透性微膠囊合成晶片之開發與即時包覆之應用 ON-DEMAND MICRO ENCAPSULATION UTILIZING ON-CHIP SYNTHESIS OF SEMI-PERMEABLE ALGINATE-PLL CAPSULES 2. 壓電式彈性駐極體與其微型能量轉換系統之應用 PIEZOELECTRIC PDMS FILMS FOR POWER MEMS		

一、參加會議經過

報告人於一百年六月初前往中國北京參加第十六屆固態感測、致動與微系統國際學術研討會，今年的會議共收到來自近四十個國家總計一千六百多篇的論文摘要，在四天的議程當中，針對所選出的七百多篇論文(接受率約百分之四十五)，分別以專題演講、報告、與海報發表的形式進行研討，有一千多位相關領域的研究人員出席。這次大會中來自台灣的論文有數十篇(其中又以本校國立清華大學的論文數量最多)，以數量來看在與會國家中名列前茅，研究品質比起歐、美、日等先進國家也毫不遜色。報告人在這次會議中所發表了兩篇論文，主要介紹本研究團隊所開發，具多步驟藻酸鈣-聚離胺酸半透性微膠囊合成功能之生醫晶片，與其在細胞與藥物即時包覆之應用。利用這套系統可以在微尺度下即時依需要合成半透性膠囊，對細胞反應監測與藥物傳輸控制有極大的幫助。另外也介紹了壓電式彈性駐極體與其微型能量轉換系統之應用，我們開發了一套簡單有效的製程，可將彈性材料透過高壓充電的方式賦予其壓電特性，可有效與現存的微系統製程整合，提供優異的電能與機械能轉換效果，將廣泛應用於壓力感測與能量轉換等各項應用，兼具學術與應用價值。除了論文的發表之外，報告人也參與大會安排的專題演講與口頭報告、並利用時間觀摩了會場所陳列的海報，透過討論和出席的各國研究人員，針對磁性奈微結構、微流體與液滴系統、與藥物釋放系統的設計、製程、與應用、微型能源系統等相關課題進行交流，在四天的議程內大量攝取研究所需的養分，並獲得相當多的啟發與靈感，這對報告人執行進行中的各項計畫都有相當大的助益。

二、與會心得

這項會議每兩年舉辦一次，今年正好是第三十年，也是第一次在中國舉辦，並且是規模最盛大的一次。這項會議有較多的口頭報告論文，提供了新生代研究生與學者們展現與交流成果的機會，從這些報告中可看出此一領域仍不斷蓬勃發展。台灣學者在微機電系統領域的研究成果一直是有目共睹的，以數量來看在與會國家中名列前茅，研究品質比起歐、美、日等先進國家也毫不遜色。相較之下日本研究團

隊值得我們學習的是其長期的投入，與因此而產生的成熟工藝與系統完整度，在實用性方面的表現最為傑出。不過這次因震災與海嘯的緣故，參加的人數相對減少。美國研究團隊值得我們學習的則是其源源不絕的創意，與龐大研究組織與資源的分配與應用，以及將成果商品化的優越能力，這次與會者不只來自大學與研究單位，也有很多業者參加。在與會的七百多篇論文當中，有相當多是集中在幾個熱門的跨領域研究課題，即使處理的問題相同，但是因為訴求與強調的重點不同，各自所提出的作法也大異其趣。針對目前蓬勃發展的跨領域研究，研究人員除了必須具備個別領域的專業技術之外，還必須不斷的充實本身對研究課題各方面的認知，透過學習與討論，以產生周密且最佳化的方案。

三、考察參觀活動(無是項活動者略)

四、建議

這項會議每年輪流在歐、美、亞三洲舉行，很高興獲知三屆後的會議將在台灣高雄主辦，相信這對我國微機電系統研究的國際知名度將會有很大的助益。由於參加人數眾多，必須有能容納上千人的國際會議廳，與旅館及餐廳等相關配合，懇請國科會與各相關單位提供必要支援以辦好這項會議，將能有效提升我國的知名度與形象。

五、攜回資料名稱及內容

近年來大會已不主動提供厚重的會議論文集和光碟資料片，而是改發載有完整會議資料的隨身碟，大大降低了攜帶的負擔與使用上的不便。

六、其他

這是報告人第四次有機會參訪北京這個城市，先前都是單純與北京清大工物系交流，這次才有較多時間與機會體驗北京這個城市的生活，感謝國科會與清大校方的補助報告人才能順利成行並有豐富的收穫。

附件：論文海報兩份。

Microfluidics**W3P.057****A CELL ELECTROPORATION AND VIABILITY MONITORING CHIP USING A SINGLE CHANNEL WITH MULTIPLE ELECTRIC FIELD ZONES**

Min-Ji Kim, Taeyoon Kim, and Young-Ho Cho

Cell Bench Research Center, Daejeon, Republic of Korea

2200

W3P.058**SPECIFIC AND LABEL-FREE IMMUNOGLOBULIN G ANTIBODY DETECTION USING NANOPOROUS HYDROGEL PHOTONIC CRYSTALS**Eunpyo Choi¹, Yuri Choi², and Jungyul Park^{1,2*}¹*Department of Mechanical Engineering, Sogang University, Seoul, Korea*²*Interdisciplinary Program of Integrated Biotechnology, Sogang University, Seoul, Korea*

2203

W3P.059**A SUBMERSIBLE PIEZORESISTIVE MEMS LATERAL FORCE SENSOR FOR CELLULAR BIOMECHANICS APPLICATIONS**

M. Gnerlich, S.F. Perry, S. Tatic-Lucic

Lehigh University, Bethlehem, PA, USA

2207

W3P.060**MANIPULATION OF ELECTRICAL CHARGE OF PROTEINS FOR SENSITIVE BIOSENSING USING FIELD-EFFECT TRANSISTORS**

T. Goda and Y. Miyahara

Institute of Biomaterials and Bioengineering, Tokyo Medical and Dental University

2211

W3P.061**PCR ON A PDMS-BASED MICROCHIP WITH INTEGRATED BUBBLE REMOVAL**J.M. Karlsson¹, T. Haraldsson¹, S. Laakso², A. Virtanen², M. Mäki², G. Ronan³, and W. van der Wijngaart¹¹*Microsystem Technology Lab, KTH Royal Institute of Technology, Stockholm, SWEDEN*²*Mobidiag OY, Helsinki, FINLAND*³*Farfield Group, Manchester, UNITED KINGDOM*

2215

W3P.062**TUNABLE SENSITIVITY AND LINEARITY OF SELF-ASSEMBLED CARBON NANOTUBE COMPOSITE BASED pH BIOSENSORS USING SILICA NANOPARTICLES**

Dongjin Lee and Tianhong Cui*

Department of Mechanical Engineering, University of Minnesota, Minneapolis, MN 55455, U.S.A.

2219

W3P.063**PATTERN GENERATION OF A MICROFLUIDIC-BASED BIOSENSOR TO DETECT C-REACTIVE PROTEIN USING THE COMPETITIVE PROTEIN ADSORPTION**

S. Choi, A. Lajevardi-khosh, and J. Chae

School of Electrical, Computer and Energy Engineering, Arizona State University, Tempe, Arizona, USA

2223

W3P.064**ON-DEMAND MICRO ENCAPSULATION UTILIZING ON-CHIP SYNTHESIS OF SEMI-PERMEABLE ALGINATE-PLL CAPSULES**

S.C. Chang, J.J. Wang, C.W. Chang, and Y.C. Su*

*Department of Engineering and System Science**National Tsing Hua University, Hsinchu, Taiwan*

2227

W3P.065**A WIRELESS LOVE WAVE BIOSENSOR PLATFORM FOR SIMULTANEOUS DETECTIONS OF TWO DIFFERENT BIOMOLECULES**T. Song¹, S.Y. Song², H.C. Yoon² and K. Lee¹¹*Department of Electrical and Computer Engineering, Ajou University, Suwon, S. Korea*²*Department of Molecular Science and Technology, Ajou University, Suwon, S. Korea*

2231

ON-DEMAND MICRO ENCAPSULATION UTILIZING ON-CHIP SYNTHESIS OF SEMI-PERMEABLE ALGINATE-PLL CAPSULES

S.C. Chang, J.J. Wang, C.W. Chang, and Y.C. Su*

Department of Engineering and System Science
National Tsing Hua University, Hsinchu, Taiwan

ABSTRACT

This paper presents an on-demand, multi-step synthesis scheme that is capable of forming semi-permeable microcapsules on an integrated microfluidic chip. Three-layered PDMS devices with pneumatically actuated diaphragm-valves constructed on specially designed fluidic-channels are utilized to realize the encapsulation process. In the prototype demonstration, Na-alginate droplets are metered, trapped, and then drawn into CaCl_2 droplets, while they react and form solid Ca-alginate microcapsules on the interfaces. In addition, entrapment and transfer of the resulting capsules can also be performed on the same microfluidic chip to further process Ca-alginate into semi-permeable alginate-PLL. As such, the demonstrated on-chip synthesis scheme could potentially fulfill the real-time controllability on micro-encapsulation, which is desired for a variety of biological and medical applications.

KEYWORDS

Encapsulation, Droplet, Alginate, On-Chip Synthesis

INTRODUCTION

Because of the strong application potential, considerable attention has been attracted to the development of controllable and reliable double emulsification schemes. Recently, researchers have demonstrated double emulsification in various microfluidic devices utilizing two-step breakup [1] and 3D flow focusing [2]. In addition, it has also been demonstrated that the middle liquid in a double emulsion can be further processed into a solid capsule [3]. For example, polymeric materials can be dissolved in the middle organic solvent, and solidified into microcapsules once the solvent is extracted. Meanwhile, microcapsules can also be fabricated by forming emulsion droplets with microfluidic devices first, and then collecting and transferring them into specific medium for sequential reactions on the droplet interfaces [4]. Most microfluidic emulsification utilizing passive schemes, which are capable of producing continuous droplet streams, but insufficient for adjusting droplet size and manipulating droplet movement in a real-time manner [5]. For multi-step processes such as encapsulation and sequential surface modification, off-chip operation is usually required. To address the need for real-time controllability on micro-encapsulation, this paper presents an integrated microfluidic system that could form semi-permeable micro-capsules with desired geometries and compositions on demand. Emulsion droplets functioning as templates and reactors are employed to realize the synthesis process. Devices with pneumatically actuated diaphragm-valves constructed on specially designed fluidic-channels are

utilized to control the droplets, and consequently the encapsulation process. Three accomplishments have been achieved: (1) a diaphragm-actuated emulsification and entrapment device that can produce monodisperse droplets with desired sizes, and selectively entrap droplets and solid capsules in a real-time manner; (2) a multi-step reaction scheme can be performed on droplet-in-droplet interfaces to synthesize alginate-poly-L-lysine (PLL) capsules; and (3) an active, integrated microfluidic system that can produce semi-permeable microcapsules with desired sizes and compositions on demand. Superior to the previously-reported double-emulsification and multi-step synthesis schemes, the demonstrated microfluidic devices could potentially fulfill the real-time controllability on micro-encapsulation, which is desired for a variety of applications.

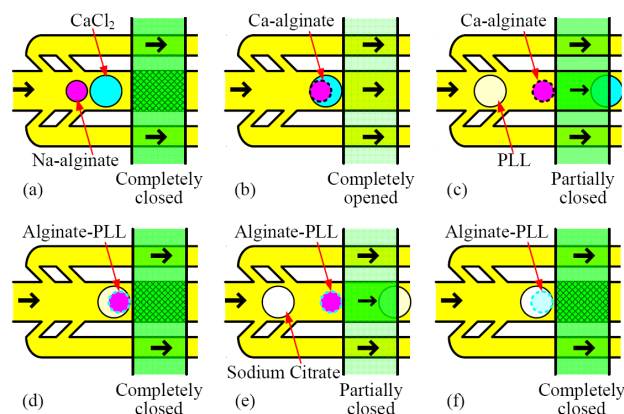
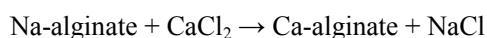


Figure 1: Schematic of the proposed encapsulation scheme

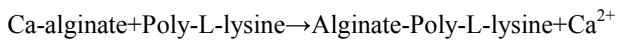
OPERATING PRINCIPLE

A schematic illustration of the proposed micro encapsulation scheme is shown in Figure 1. A three-layered microfluidic chip with pneumatically actuated diaphragm-valves built on specially designed microfluidic-channels is utilized to perform the multi-step synthesis process. The complete collapse of a diaphragm on the central flow-path stops the droplets and results in the merger into a double-emulsion structure (Figure 1-a). Two droplets containing aqueous Na-alginate and CaCl_2 solutions individually react on the interface to form a solid Ca-alginate capsule (Figure 1-b) as the following:



The diaphragm-valve is then partially opened, which allows outer un-reacted CaCl_2 solution to pass while the solid capsule remains trapped (Figure 1-c). The trapped capsule is rinsed by an incoming buffer droplet and then

re-suspended into another incoming droplet containing PLL, while the valve turns completely closed (Figure 1-d). Re-suspension of the capsules into PLL solution results in the formation of an alginate-PLL capsule due to the poly- ion complex:



Once an alginate-PLL capsule is formed, it is rinsed and then re-suspended into a droplet of sodium-citrate solution to dissolve unreacted Ca-alginate gel inside the capsule (Figure 1-e). At the end, an alginate-PLL capsule is formed with its core in liquid state, and released for sequential processing (Figure 1-f). Meanwhile, a T-junction with a diaphragm-valve mounted on its top (as shown in Figure 2) is employed to control the metering process [6].

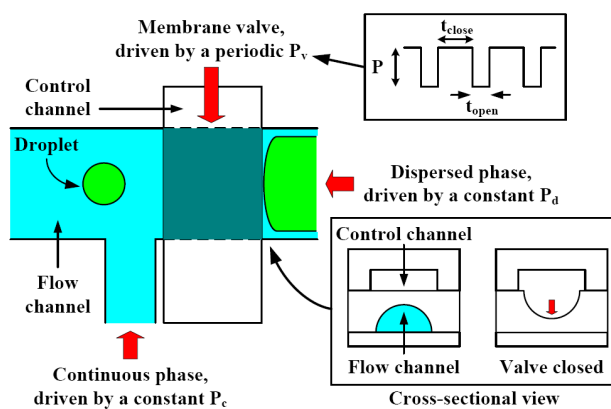


Figure 2: Schematic of the proposed metering scheme

FABRICATION PROCESSES

A 3-layered, PDMS molding and irreversible bonding process was employed to fabricate the proposed microfluidic chip, as illustrated in Figure 3. First of all, a layer of 25 μm thick positive photoresist (9260, AZ Electronic Materials) was spin-coated and patterned on top of a clean silicon wafer to fabricate the mold used for duplicating the top half of the flow channel. Afterwards, the patterned photoresist layer was baked at 120 $^{\circ}\text{C}$ for 30 min, during which the photoresist reflowed and its profile became rounded. Meanwhile, the molds used for duplicating the control channel and the bottom half of flow channel were fabricated by coating and patterning 10 μm and 100 μm thick layers of negative photoresist (SU-8, MicroChem) on top of clean silicon wafers, respectively. After the three photoresist molds were fully cured, they were placed in a desiccator under vacuum for 3 hours with a vial containing a few drops of 1H,1H,2H,2H-perfluorooctyl-trichlorosilane (Fluka) to silanize the surfaces. A mixture of 10:1 PDMS pre-polymer and curing agent (Sylgard 184, Dow-Corning) was stirred thoroughly and then degassed under vacuum to remove entrapped air bubbles. The casting and bonding process started with the deposition of a thin PDMS mixture layer on top of the top flow-channel mold. About one tenths of

the PDMS mixture was spin-coated on the mold at 2000 rpm for 30 seconds, which yielded a thickness of roughly 50 μm , and cured for 15 minutes at 85 $^{\circ}\text{C}$. Meanwhile, about half of the PDMS mixture was poured onto the control-channel mold, degassed, cured for 15 minutes at 85 $^{\circ}\text{C}$, and then peeled off from the mold. Afterwards, the control-channel layer was pressed and bonded on top of the 50 μm -thick top flow-channel layer, and left undisturbed for at least 1 hour at 85 $^{\circ}\text{C}$ for the bonding to take effect. The bonded, two-layer PDMS structure was then peeled off from the silicon wafer, and punched through with a sharp metal-tube array to fabricate the holes for multiple inlets and outlets. Meanwhile, the left PDMS mixture was poured onto the bottom flow-channel mold, degassed, cured for 1 hour at 85 $^{\circ}\text{C}$, and then peeled off from the mold. The surfaces of the two-layer PDMS structure (on the flow channel side) and the duplicated bottom flow-channel layer were then treated with a hand-held corona treater (BD-20AC, Electro-Technic Products), which ionizes surrounding air and creates localized plasma to activate the surfaces for irreversible bonding. The wire electrode was positioned approximately 3 mm above the treated surface, and scanned back and forth for 30 seconds to 1 minute, depending on the size of the surface. The corona-treated surfaces were then pressed together and left undisturbed for at least 1 hour at 85 $^{\circ}\text{C}$ for the bonding to take effect. At the end, multiple PTFE tubes were inserted into the punched holes to build the necessary interconnection for compressed-air supply and fluidic sample injection and discharge.

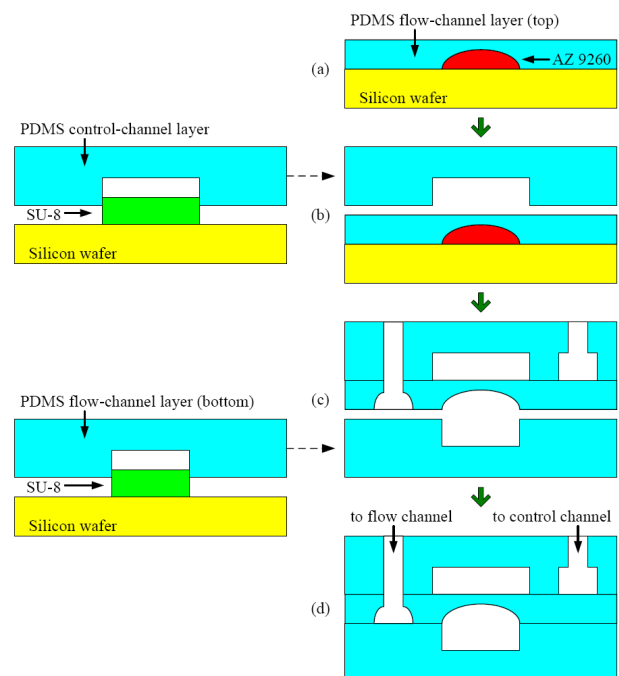


Figure 3: A 3-layered, PDMS molding and bonding process

EXPERIMENTAL DETAILS

The operation of the presented integrated system is illustrated in Figure 4. An air compressor (Model 3-4, Jun-Air) with its output set at 500 kPa was employed as the single pressure source to drive the operation. Each liquid sample was stored in a separate plastic container, which was fed with pressurized air from the top to drive the sample flowing through the bottom tube and into the downstream microfluidic devices. The actual driving pressure applied on each container was adjusted independently by a separate pressure regulator (IR1000-01G, SMC). Meanwhile, the actuation of each diaphragm valve was controlled independently by a separate electromagnetic valve (VK332-5G-M5, SMC), whose action was governed by a computer controlled relay circuitry. A governing program developed and executed under a software environment (LabVIEW, National Instruments), cooperating with a set of hardware adapter and connector (PCI-6220 + CB-68LP), was employed to coordinate the actuation of the prototype system. As such, the operation can be either pre-programmed or responding to demand in a real-time manner. The emulsification and encapsulation processes were observed under an optical microscope and the images were recorded using either a standard CCD camera (SSC-DC80, SONY) or a high-speed digital camera (SR series, KODAK Motion Corder Analyzer), which was also connected to the computer. The resulting droplets and capsules were driven into a 200 μm deep reservoir, where droplets and capsules would be perfect spheres without unwanted deformation. The volumes of the resulting droplets and capsules were then estimated based on the observed spherical diameters.

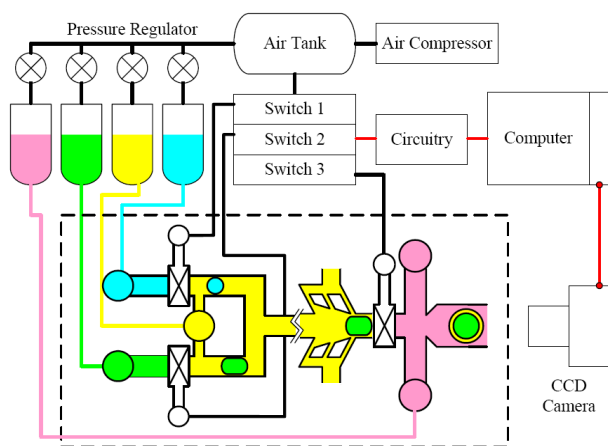


Figure 4: Experimental setup of the encapsulation scheme

RESULTS AND DISCUSSION

The injection of a relatively small Na-alginate droplet into a relatively large CaCl_2 droplet is the most critical step in the proposed encapsulation process. Figure 5 shows images of two injection sequences with Na-alginate droplets of 150 and 100 μm in diameter. Concentration (and consequently the viscosity) of the left-hand side Na-alginate droplet is found to dramatically affect the shape of the resulting Ca-alginate capsule.

With a Na-alginate concentration of 1 wt%, the shapes of the resulting Ca-alginate capsules, as shown in Figure 5, are sickle like. Since the viscosities of Na-alginate and calcium chloride solutions are around the same order, in these cases the Na-alginate droplets are greatly deformed by the flow inside the calcium chloride droplets. In around 10 (Figure 5-a) and 5 (Figure 5-b) milliseconds, the interfaces between Na-alginate and calcium chloride droplets solidify and Ca-alginate capsules are formed. However, the application of these capsules would be limited because of their sickle like shapes. Fortunately, it is also found that with a concentration higher than 3 wt%, the viscosity of a Na-alginate solution becomes much higher than that of a calcium chloride solution with a concentration remaining at 1.5 wt%. When a highly viscous Na-alginate droplet is drawn into a dilute calcium chloride droplet (as illustrated later in Figure 6), it remains intact and solidifies to form a circular-shaped Ca-alginate capsule.

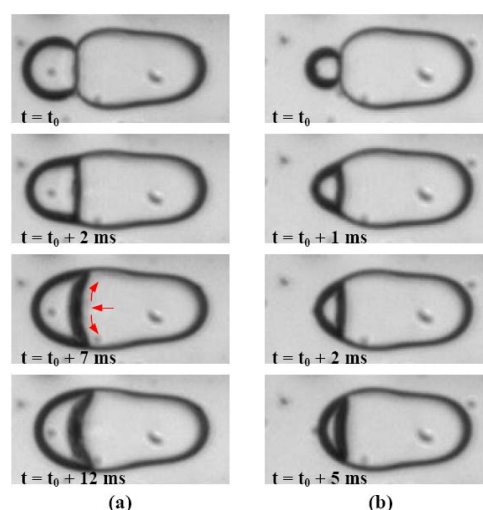


Figure 5: Captured sequences of droplet coalesce with droplet diameters of 150 μm (a) and 100 μm (b)

Controlled encapsulation was successfully demonstrated using the fabricated microfluidic devices, and a captured encapsulation sequence is shown in Figure 6. First of all, Na-alginate and CaCl_2 droplets are metered and selectively trapped in front of a collapsed diaphragm, whose movement further results in the merger of droplets into a double-emulsion structure. The retreat of the diaphragm (Figure 6-b~c) causes a negative pressure gradient, which sucks in the liquids and in turn accelerates the draining of the liquid film between the trapped droplets. Meanwhile, the re-collapse of the diaphragm (Figure 6-e~f) remains the double-emulsion structure trapped in front of the diaphragm. In the demonstration, overall three solid Ca-alginate capsules are formed in a CaCl_2 droplet (Figure 6-g) using the same approach. Afterwards, the diaphragm valve is partially opened. The solid capsules remain trapped (Figure 6-h~i), while un-reacted CaCl_2 solution is dragged away by the con-

tinuous-phase flow. The partial collapse of the diaphragm, which can be adjusted by the applying pressure, is estimated to leave a gap of about 50 μm in width and 10 μm in height. Once un-reacted solution is largely dragged away, the solid capsules are pushed back by the complete collapse of the diaphragm (Figure 6-j). Furthermore, rinse and re-suspension of the solid capsules are also demonstrated by the coalescence with droplets of buffer and PLL solutions, respectively. Finally, re-suspension of the Ca-alginate capsules into a PLL-solution droplet results in the formation of alginate-PLL capsules (Figure 6-k~l). Once alginate-PLL capsules are formed, they are rinsed and then re-suspended into a droplet of sodium-citrate solution to dissolve unreacted Ca-alginate gel inside the capsule. The semi-permeability and flexibility of the resulting liquid-cored alginate-PLL capsules is tested by re-suspending the capsules into a droplet with a relatively low osmotic pressure. To facilitate the observation on capsule deformation, particles of 5 μm in diameter are dispersed in Na-alginate droplets at the beginning and eventually deposited on the surfaces of the capsules. It is observed that the capsule expands and therefore the distance between two specific deposited particles increases over time. The capsule becomes more transparent while it expands. Meanwhile, the capsule shrinks in case it is re-suspended into a droplet with a relatively high osmotic pressure. The expansion and shrinkage can be reversed and repeated if the droplet is re-suspended into corresponding droplets. In addition, an alginate-PLL capsule with liquid core can be contracted or stretched when forces applying on it.

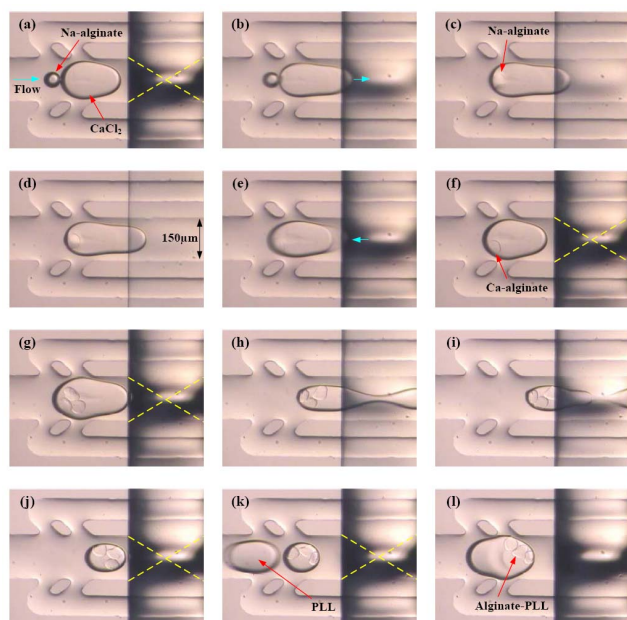


Figure 6: A captured controlled encapsulation sequence

CONCLUSION

We have successfully demonstrated an on-demand,

multi-step synthesis scheme that is capable of forming semi-permeable micro-capsules on an integrated microfluidic chip. Emulsion droplets functioning as templates and reactors are employed to realize the multi-step synthesis process. Three-layered PDMS micro-devices with diaphragm-valves constructed on specially designed fluidic-channels are utilized to control the droplets, and consequently the encapsulation process. In the prototype demonstration, a governing computer program cooperating with a set of control hardware was employed to coordinate the actuation of the system. Relatively small Na-alginate droplets are metered, trapped, and then injected into relatively large CaCl_2 droplets, while they react and form solid Ca-alginate micro-capsules on the interfaces. In addition, entrapment and transfer of the resulting capsules can also be performed on the same microfluidic system to further react Ca-alginate into semi-permeable alginate-PLL. It has been demonstrated that: (1) both emulsion droplets and solid capsules could be manipulated; (2) multi-step reactions could be performed on droplet-in-droplet interfaces to synthesize alginate-PLL capsules; and (3) on demand, controlled encapsulation could be achieved on one single microfluidic system.

ACKNOWLEDGEMENTS

This work was supported in part by the National Science Council of Taiwan under Contract No. NSC 99-2628-E-007-028. The demonstrated chips were fabricated in the ESS Micro-fabrication Lab. at National Tsing Hua University, Taiwan.

REFERENCES

- [1] S. Okushima, T. Nisisako, T. Torii, and T. Higuchi, "Controlled production of monodisperse double emulsions by two-step droplet breakup in microfluidic devices", *LANGMUIR* **20**, 9905–8, 2004
- [2] A. Utada, E. Lorenceau, D. Link, P. Kaplan, H. Stone, and D. Weitz, "Monodisperse double emulsions generated from a microcapillary device", *SCIENCE* **308**, 537-41, 2005
- [3] C. Liao and Y. Su, "Formation of biodegradable microcapsules utilizing 3D, selectively surface-modified PDMS microfluidic devices", *BIOMED MICRODEVICES* **12**, 125-33, 2010
- [4] Y. Morimoto, W. Tan, Y. Tsuda, and S. Takeuchi, "Monodisperse semi-permeable microcapsules for continuous observation of cells", *LAB CHIP* **9**, 2217-23, 2009
- [5] M. Joanicot and A. Ajdari, "Droplet control for microfluidics", *SCIENCE* **309**, 887-8, 2005
- [6] B. Lin and Y. Su, "On-demand liquid-in-liquid droplet metering and fusion utilizing pneumatically-actuated membrane valves", *J MICROMECH MICROENG* **18**, #115005, 2008

CONTACT

* Y.C. Su, Tel: 886-3-574-2374; ycsu@ess.nthu.edu.tw

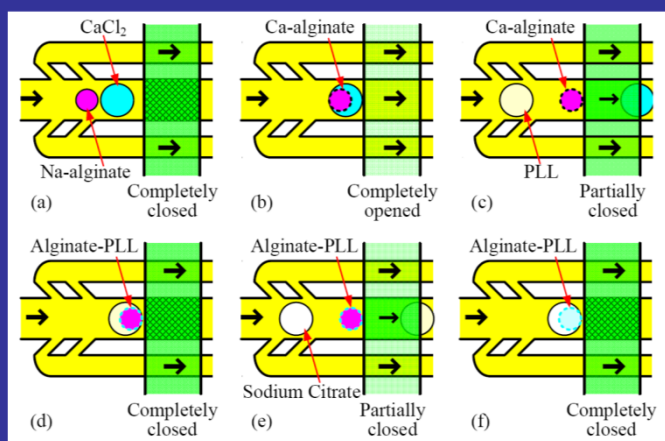
ON-DEMAND MICRO ENCAPSULATION UTILIZING ON-CHIP SYNTHESIS OF SEMI-PERMEABLE ALGINATE-PLL CAPSULES



S.-C. Chang, J.-J. Wang, C.-W. Chang and Y.-C. Su
Department of Engineering & System Science
National Tsing Hua University, Taiwan

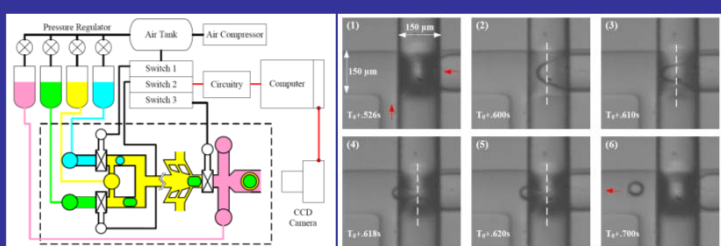
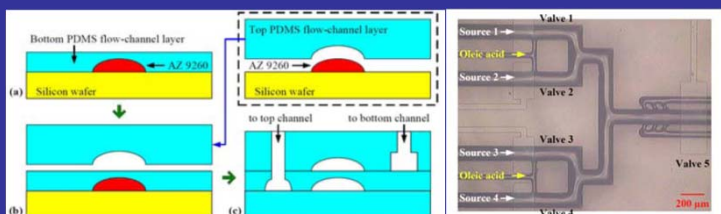
Operating Principle

- The **complete collapse** of a diaphragm stops the droplets and results in a **double emulsion**
- Droplets containing **Na-alginate** and **CaCl₂** react on the **interface** to form a **Ca-alginate capsule**
- The diaphragm-valve is **partially opened**, which allows outer **un-reacted CaCl₂** to pass
- The trapped capsule is **rinse**d by an incoming buffer droplet and then **re-suspended** into **PLL**
- Once an **alginate-PLL capsule** is formed, it is re-suspended into **sodium-citrate** to dissolve **unreacted Ca-alginate gel** inside the capsule
- An alginate-PLL capsule **with liquid core** is formed and **released** for sequential processing



Experimental

- A **PDMS molding** and irreversible **bonding** process is employed to fabricate the devices
- A **LabVIEW** program cooperating with a set of hardware adapter, circuitry, and electromagnetic switches is employed to **coordinate the operation**
- 4 aqueous solutions (**sodium alginate**, **calcium chloride**, **poly-L-lysine**, and **sodium citrate**) were dispersed into the continuous-phase **oleic acid**

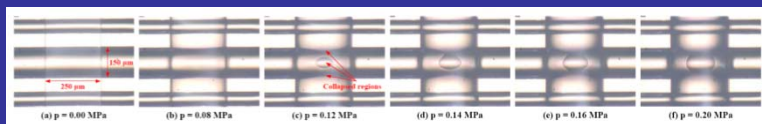


Acknowledgement

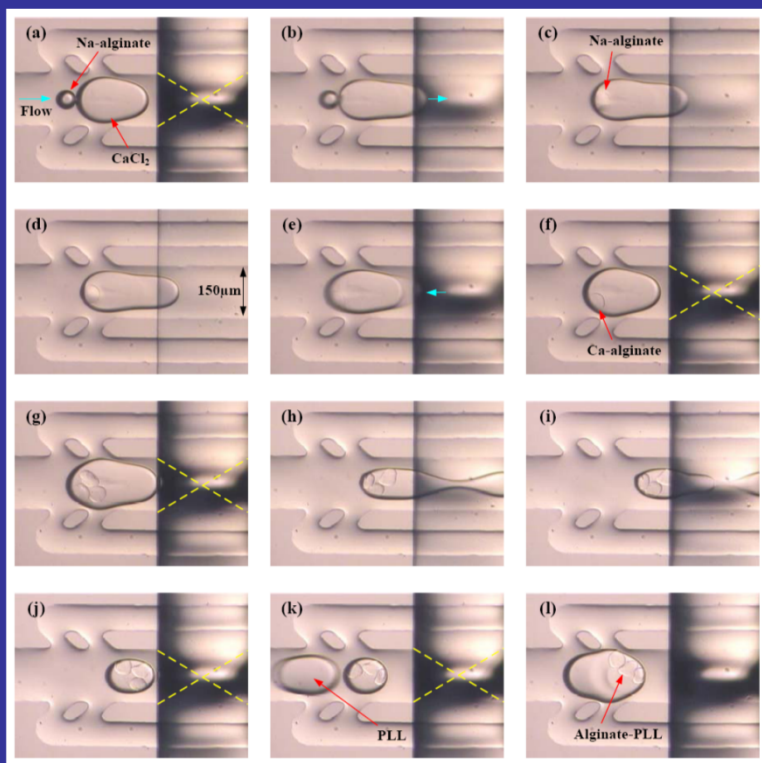
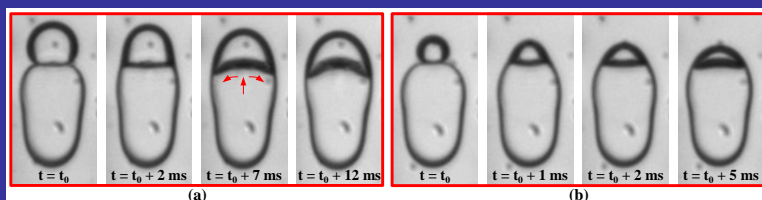
This work is supported by the National Science Council of Taiwan (NSC 99-2628-E-007-028)

Results

- With a deformable area of **150 μm x 250 μm** and a diaphragm thickness of **25 μm** , the diaphragm collapses with the increase of **pneumatic pressure**



- The **injection** of a small Na-alginate droplet into a large CaCl₂ droplet in the **encapsulation** process



Conclusions

- An **on-demand, multi-step** synthesis scheme that is capable of forming **semi-permeable microcapsules** on an **integrated** microfluidic chip
- Na-alginate** droplets are metered, trapped, and then drawn into **CaCl₂** droplets, while they react and form solid **Ca-alginate** microcapsules on the interfaces
- In addition, **entrapment** and **transfer** of the resulting capsules can also be performed on the same microfluidic chip to further process Ca-alginate into **semi-permeable alginate-PLL**
- The demonstrated on-chip synthesis scheme could potentially fulfill the **real-time controllability on micro-encapsulation**, which is desired for a variety of biological and medical applications

W3P.162	<p>A NOVEL ASSEMBLY METHOD FOR MICRO DIRECT METHANOL FUEL CELLS USING MULTI-LAYER BONDING TECHNIQUE Y.M. Zhu, X.H. Wang, Y.A. Zhou, L.T. Liu <i>Institute of Microelectronics, Tsinghua University, Beijing, China</i> <i>Tsinghua National Laboratory for Information Science and Technology, Beijing, China</i></p> <p>.....2618</p>
W3P.163	<p>PIEZOELECTRIC PDMS FILMS FOR POWER MEMS J.J. Wang, J.M. Hsieh, R.W. Tsai, and Y.C. Su <i>Department of Engineering and System Science</i> <i>National Tsing Hua University, Hsinchu, Taiwan</i></p> <p>.....2622</p>
W3P.164	<p>AGING CHARACTERISTICS OF ELECTRET USED IN A VIBRATION-BASED ELECTROSTATIC INDUCTION ENERGY HARVESTER Y. Wada¹, Y. Hamate¹, S. Nagasawa¹, H. Kuwano¹ ¹<i>Tohoku University, Sendai, Miyagi, JAPAN</i></p> <p>.....2626</p>
W3P.165	<p>VIBRATION-DRIVEN MEMS ENERGY HARVESTER WITH VACUUM UV-CHARGED VERTICAL ELECTRETS K. Yamashita^{1,2*}, M. Honzumi^{1,2}, K. Hagiwara^{1,3}, Y. Iguchi³, and Y. Suzuki^{1,2} ¹<i>Dept. of Mechanical Engineering, The University of Tokyo,</i> ²<i>G Device Center, BEANS Project,</i> ³<i>NHK Science & Technology Research Laboratories</i></p> <p>.....2630</p>
W3P.166	<p>ELECTRET BASED ENERGY HARVESTER USING A SHARED SI ELECTRODE K. Fujii¹, T. Toyonaga^{1,2}, T. Fujita^{1,2}, Y. G. Jiang², K. Higuchi² and K. Maenaka^{1,2} ¹<i>University of Hyogo, Himeji, Hyogo, Japan</i> ²<i>JST ERATO Maenaka Human-Sensing Fusion Project, Himeji, Hyogo, Japan</i></p> <p>.....2634</p>
W3P.167	<p>INCREASED-BANDWIDTH, MEANDERING VIBRATION ENERGY HARVESTER D. F. Berdy^{1,3}, B. Jung¹, J. F. Rhoads^{2,3}, and D. Peroulis^{1,2,3} ¹<i>School of Electrical and Computer Engineering, Purdue University, West Lafayette, IN, 47907, USA</i> ²<i>School of Mechanical Engineering, Purdue University, West Lafayette, IN, 47907, USA</i> ³<i>Birck Nanotechnology Center, Purdue University, West Lafayette, IN, 47907, USA</i></p> <p>.....2638</p>
W3P.168	<p>FABRICATION OF HIGHLY DIELECTRIC NANO-BATIO₃/EPOXY-RESIN COMPOSITE PLATE HAVING TRENCHES BY MOLD CASTING AND ITS APPLICATION TO CAPACITIVE ENERGY HARVESTING M. Suzuki¹, N. Matsushita¹, T. Hirata¹, R. Yoneya¹, J. Onishi¹, T. Wada¹, T. Takahashi¹, T. Nishida², Y. Yoshikawa², and S. Aoyagi¹ ¹<i>Kansai University, Osaka, Japan</i> ²<i>ROHM Co., Ltd., Kyoto, Japan</i></p> <p>.....2642</p>
W3P.169	<p>EFFICIENT ENERGY HARVESTING FROM HUMAN MOTION USING WEARABLE PIEZOELECTRIC SHELL STRUCTURES Boram Yang and Kwang-Seok Yun <i>Department of Electronic Engineering, Sogang University, Seoul, Korea</i></p> <p>.....2646</p>
W3P.170	<p>A VIBRATION-BASED ELECTROMAGNETIC ENERGY HARVESTER SYSTEM WITH HIGHLY EFFICIENT INTERFACE ELECTRONICS Arian Rahimi^{1,2}, Özge Zorlu², Ali Muhtaroglu³, and Haluk Külah^{1,2} ¹<i>METU, Department of Electrical and Electronics Engineering, Ankara, Turkey</i> ²<i>METU-MEMS Research and Application Center, Ankara, Turkey</i> ³<i>METU-NCC, Department of Electrical and Electronics Engineering, Güzelyurt, Mersin 10 Turkey</i></p>

PIEZOELECTRIC PDMS FILMS FOR POWER MEMS

J.J. Wang, J.M. Hsieh, R.W. Tsai, and Y.C. Su
 Department of Engineering and System Science
 National Tsing Hua University, Hsinchu, Taiwan

ABSTRACT

We have successfully demonstrated the fabrication of piezoelectric PDMS films utilizing casting, stacking, and micro plasma discharge processes. To realize electromechanical sensitivity, PDMS structures with micrometer-sized cells are implanted with positive and negative charges on the opposite internal surfaces of each cell, which behaves just like a dipole. In the prototype demonstration, multilayer PDMS films with inner cells of $50 \times 50 \times 50 \mu\text{m}^3$ are fabricated and charged under electric fields up to 40 MV/m. The resulting cellular PDMS films show an elastic modulus of at least 12% lower than solid ones and a piezoelectric coefficient (d_{33}) up to 182 pC/N, which is about 10 times higher than that of common piezoelectric polymers (e.g., PVDF). As such, the demonstrated piezoelectric PDMS films could serve as soft and sensitive electromechanical transducers, which are desired for a variety of sensor and energy harvesting applications.

KEYWORDS

Micro Plasma Discharge, Cellular Polymer, Energy Harvesting, Piezoelectric Material

INTRODUCTION

Electrets, the electrostatic equivalents of permanent magnets, are dielectric materials that have quasi-permanent electric charges or dipole polarization [1]. They function as permanent sources of electric fields, which are employed to act on objects, interact with other physical fields, or induce AC current. Conventionally, electrets are made up of certain dielectrics with charges stored mostly on their surfaces. The electret effects are usually resulted from dipolar polarization, charge displacement inside molecules or domains, and the formation of spatial or surface charges. To fabricate electrets, dielectrics are placed in electric fields and subjected to additional physical actions, which either reduce dipolar relaxation or accelerate the migration of charged particles.

Ferroelectrets, which are polymer foams with bipolar charges stored in each cell, have recently been demonstrated to be highly efficient in charge storage and showing unexpected piezoelectricity [2-4]. Surprisingly, completely non-polar materials without any molecular dipoles can behave almost like ferroelectrics. Unfortunately, it is difficult to control the sizes and geometries of ferroelectrets, or integrate them with microsystems. To address these fabrication issues, this paper presents controlled foam forming, casting, stacking, surface modification, and micro plasma discharge processes that could readily produce piezoelectric PDMS electrets with desired geometries and properties. In addition, these

processes should be compatible with common MEMS fabrication. As such, the proposed piezoelectric PDMS electrets could be readily integrated and serve as soft and sensitive electromechanical transducers, which are desired for a variety of MEMS sensor and energy harvesting applications.

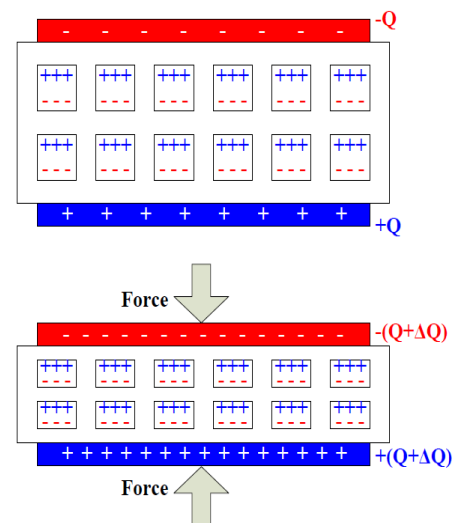


Figure 1: Schematic of electret structure and piezoelectricity

OPERATING PRINCIPLE

To obtain electromechanical sensitivity, multilayer PDMS structures with micrometer-sized cells are implanted with positive and negative charges on the opposite internal surfaces of each cell, which behaves just like a dipole. The charging of the cells is realized by placing cellular PDMS films in strong electric fields, which eventually cause the air inside the cells to break down. When performed between two parallel plate electrodes, the breakdown criteria can usually be predicted by the Paschen's law [5], while fails for gaps smaller than 10 μm in air at one atmosphere [6]. Generally, the required breakdown fields are higher for smaller cells. Once broken down, micro plasma discharges are generated inside the cells and then self extinguished because of the deposition of charges on the internal surfaces of each cell. The charged PDMS foams are flexible and highly polarized. Up-on the application of mechanical or electrical stresses, the quasi-dipoles inside PDMS electrets change their dimensions and dipole moments, which results in the desired piezoelectricity as illustrated in Figure 1. The application of a force to a PDMS electret is expected to induce additional charges on the top and bottom electrodes. Overall, the piezoelectricity of a cellular PDMS structure is dependent on its porosity, elastic modulus, cell size, and surface charge density.

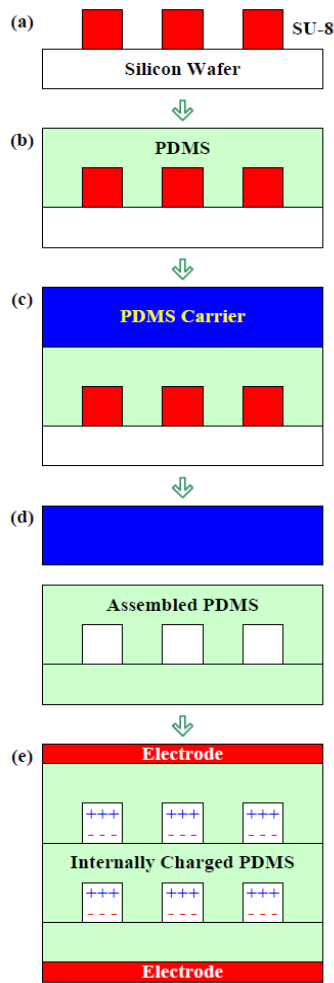


Figure 2: Schematic of the proposed fabrication process

FABRICATION PROCESSES

Figure 2 illustrates the fabrication of multi-layer piezoelectric PDMS structures. First of all, a layer of $50\text{ }\mu\text{m}$ thick photoresist (SU-8) was spin-coated and patterned on top of a clean silicon wafer to fabricate the mold used for duplicating the cellular structures. The casting and stacking process started with the deposition of a thin ($\sim 100\text{ }\mu\text{m}$) PDMS mixture layer on top of the mold, and cured for 1 hour at 85°C . Afterwards, the top surface of the cured PDMS layer was treated by 1H,1H,2H,2H-per-fluorooctyl-trichlorosilane [7]. A 2 mm thick PDMS layer, which functioned as a reusable transferring carrier, was then casted on top of the surface-treated structure. The thin PDMS structure was peeled off from the mold, and transferred to a spin-casted, blank PDMS layer of $50\text{ }\mu\text{m}$ thick. Since the bonding strength between native PDMS surfaces is higher than that between native and treated surfaces, casted PDMS layer was separated from the carrier. Multi-layer structures can be constructed by repeating the casting and stacking processes. In this work, a stack of two layers of inner cells was formed. The overall thickness of the assembled PDMS structure can be as low as $250\text{ }\mu\text{m}$. A resulting assembled structure of $400\text{ }\mu\text{m}$ is shown in Figure 3. The size of the inner cells is

$50\times 50\times 50\text{ }\mu\text{m}^3$, and the distance between cells is $50\text{ }\mu\text{m}$. In addition to closed cell structures, open cell structures were fabricated and characterized as well. The geometry is shown in Figure 4. With open cell structures, surface modification and deposition can be realized. It is expected that the deposition of extra semi-crystalline polymers or dielectric nanoparticles, which are capable of storing charges stably, could further improve the piezoelectricity of fabricated cellular PDMS structures.

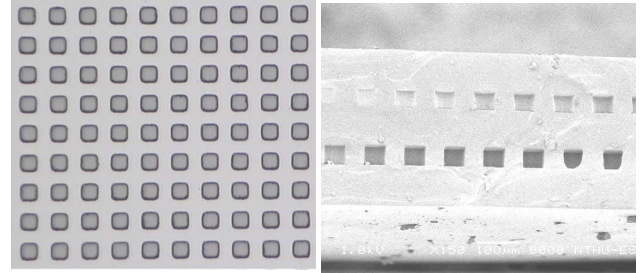


Figure 3: Optical and SEM micrographs of a fabricated cellular PDMS structure

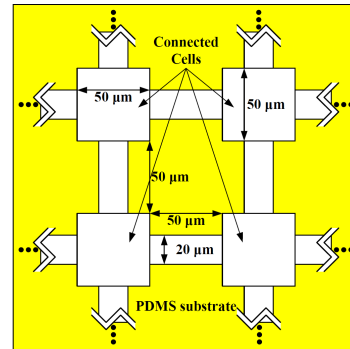


Figure 4: Geometry of open cell structure

In current work, the fabricated cellular PDMS films have an area of $3\text{ cm} \times 3\text{ cm}$, and a thickness of roughly $250\text{ }\mu\text{m}$. The PDMS films were coated with electrodes on their top and bottom surfaces, and charged under strong electric fields. In our trials, charge voltages up to 10 kV , which corresponds to an electric field strength of 40 MV/m , were employed to ionize the air within the cells. Once the required breakdown field is reached, a self-extinguishing micro discharge was ignited in a cell, accompanied by the emission of a short light pulse and by the transfer of charges across the cell. Charges were accelerated and implanted onto the inner surfaces. In our trials, charge voltages were triangular waves with amplitude between 1 and 10 kV , and frequencies of less than 0.2 Hz . Meanwhile, the charged PDMS films were heated up to 140°C . By repeatedly charging the samples at high temperatures, less stable charges are more likely to be expelled from the surfaces and replaced with more stable charges. Once being internally charged, the cellular PDMS films behave like soft and sensitive piezoelectric materials that can be used to interconvert signals between acoustical and electrical or mechanical and electrical.

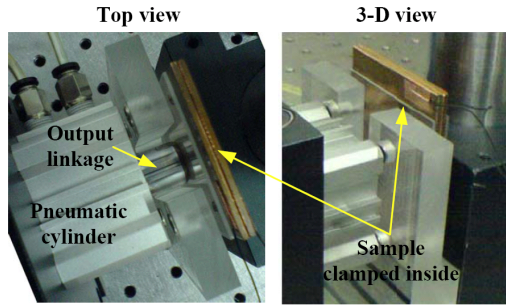


Figure 5: Experimental setup for piezoelectricity characterization

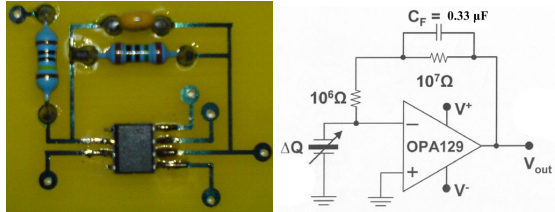


Figure 6: Photograph of an employed charge amplifier and its equivalent circuit

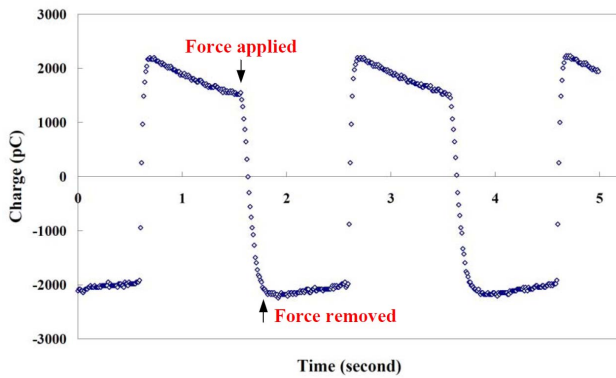


Figure 7: Measured charge variation of a closed-cell type PDMS structure

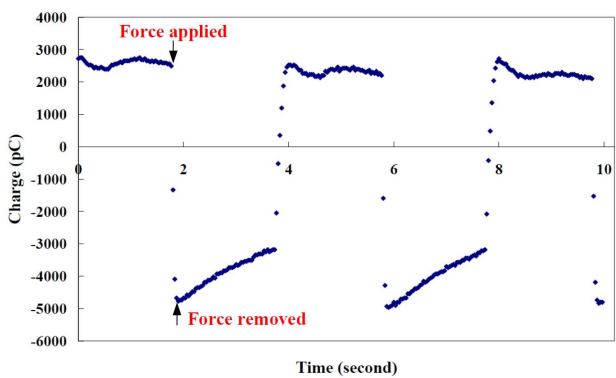


Figure 8: Measured charge variation of an open-cell type PDMS structure

EXPERIMENTAL AND RESULTS

The piezoelectricity of fabricated and charged PDMS films were characterized using a setup illustrated in Figure 5. A force is applied periodically by a pneumatic cylinder to the tested sample, which is clamped on a

customized fixture. The elastic modulus of the cellular PDMS films is estimated to be at least 12% lower than that of solid ones, while the measured value is 510 kPa. Meanwhile, electrodes of the tested sample were connected to a charge amplifier (as shown in Figure 6), which converts sensed charge variations into amplified voltage outputs. In our trials, a 40 N force, which corresponds to an air pressure of 1 kgf/cm², was applied on each of the 3 cm × 3 cm large tested sample. Under this condition, a 1 mV voltage output is estimated to indicate an 82.3 pC charge induction on the electrodes. Figure 7 shows the measured piezoelectricity of a closed-cell type PDMS structure. The application of a 40 N force actually results in a 4120 pC charge variation, which corresponds to a piezoelectric coefficient (d_{33}) of 103 pC/N. As illustrated in Figure 8, a open-cell type sample shows a 7310 pC charge variation, which corresponds to a piezoelectric coefficient (d_{33}) of 182 pC/N, which is about 10 times higher than that of common piezoelectric polymers (e.g., PVDF). Meanwhile, the elastic modulus of the open-cell type samples is estimated to be at least 32% lower than that of solid ones. It was observed during the charging process that the required breakdown field for closed-cell type samples was higher than that for open-cell type samples. Under the same electric field, the resulting breakdown current and therefore the piezoelectricity of an open-cell type sample is distantly higher than that of a closed-cell type one.

One severe drawback of the presented fabrication scheme is that the life-time of the implanted charge is mostly in the range of days to weeks. Therefore, the resulting piezoelectricity lasted only for a relatively short period of time. This issue could potentially be solved by the deposition of extra semi-crystalline polymers or dielectric nanoparticles on cell surfaces. As already mentioned, surface deposition of materials capable of storing charges stably could improve the piezoelectricity and its life-time. Currently we are studying the effects caused by the deposition of semi-crystalline polypropylene (PP) and polytetrafluoroethylene (PTFE). Open cell structures are filled with polymer solutions, and eventually deposited with thin polymer layers once solvents evaporated. Furthermore, mainly by increasing the number of layer of the cellular structures and the field for charge implantation, the resulting piezoelectricity can be improved as well.

CONCLUSION

This paper presents the fabrication of piezoelectric PDMS structures utilizing casting, stacking, and micro plasma discharge processes. In order to acquire electro-mechanical sensitivity, PDMS structures with micrometer-sized closed and open cells are implanted with positive and negative charges on the opposite internal surfaces of each cell, which behaves just like a dipole. Upon the application of mechanical or electrical stresses, the quasi-dipoles inside a cellular PDMS structure change their dimensions and dipole moments as well, which results in the desired piezoelectricity. In the prototype

demonstration, multilayer PDMS films with inner cells of $50 \times 50 \times 50 \mu\text{m}^3$ are fabricated and charged under electric fields up to 40 MV/m. The resulting cellular PDMS films show an elastic modulus of up to 32% lower than solid ones and a piezoelectric coefficient (d_{33}) up to 182 pC/N, which is about 10 times higher than that of common piezoelectric polymers (e.g., PVDF). It was observed during the charging process that the required breakdown field for closed-cell type samples was higher than that for open-cell type samples. Under the same electric field, the resulting breakdown current and therefore the piezoelectricity of an open-cell type sample is distinctly higher than that of a closed-cell type one. Meanwhile, the resulting piezoelectricity lasted only for a relatively short period of time. This issue could potentially be solved by the deposition of extra semi-crystalline polymers or dielectric nanoparticles on cell surfaces. It is expected that surface deposition of materials capable of storing charges stably could improve the piezoelectricity and its life-time. Mainly by increasing the number of layer of the cellular structures and the field for charge implantation, the resulting piezoelectricity can be improved as well. As such, the demonstrated piezoelectric PDMS films could serve as soft and sensitive electromechanical transducers, which are desired for a variety of sensor and energy harvesting applications.

ACKNOWLEDGEMENTS

This work was supported in part by the National Science Council of Taiwan under Contract No. NSC 99-2628-E-007-028. The demonstrated chips were fabricated in the ESS Micro-fabrication Lab. at National Tsing Hua University, Taiwan.

REFERENCES

- [1] V.N. Kestelman, L.S. Pinchuk, and V.A. Goldade, *Electrets in Engineering*, Kluwer, 2000
- [2] S. Bauer, G.M. Sessler, and R. Gerhard-Multhaupt, "Ferroelectrics: Soft Electroactive Foams for Transducers" *Physics Today*, 57, pp. 37-43, 2004
- [3] R. Gerhard-Multhaupt, "Less can be More: Holes in Polymers lead to a New Paradigm of Piezoelectric Materials for Electret Transducers" *IEEE Transactions on Dielectrics and Electrical Insulation*, 9, pp. 850-859, 2002
- [4] M. Lindner, S. Bauer-Gogonea, S. Bauer, M. Paajanen, and J. Raukola, "Dielectric Barrier Microdischarges: Mechanism for the Charging of Cellular Piezoelectric Polymers" *IEEE Transactions on Dielectrics and Electrical Insulation*, 11, pp. 255-263, 2004
- [5] M.S. Naidu and V. Kamaraju, *High Voltage Engineering*, McGraw-Hill, 1996
- [6] E. Hourdakis, B. Simonds, and N.M. Zimmerman, "Submicron Gap Capacitor for Measurement of Breakdown Voltage in Air" *Review of Scientific Instruments*, 77, 034702, 2006
- [7] M. Zhang, J. Wu, L. Wang, K. Xiao, and W. Wen, "A

Simple Method for Fabricating Multi-Layer PDMS Structures for 3D Microfluidic Chips" *Lab on a Chip*, 10, 1199-1203, 2010

CONTACT

* Y.C. Su, Tel: 886-3-574-2374; ycsu@ess.nthu.edu.tw

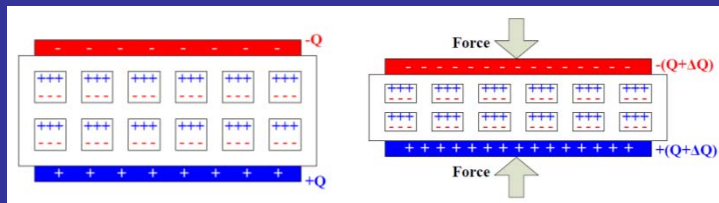
PIEZOELECTRIC PDMS FILMS FOR POWER MEMS



J.-J. Wang, J.-M. Hsieh, R.-W. Tsai and Y.-C. Su
Department of Engineering & System Science
National Tsing Hua University, Taiwan

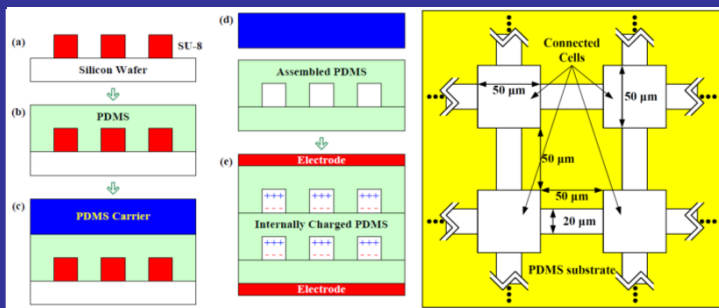
Abstract

- PDMS films function as **piezoelectric** materials that are capable of converting **mechanical movement** into **electric potential**
- Multilayer** PDMS structures with inner cells of $50 \times 50 \times 50 \mu\text{m}^3$ are fabricated and charged under electric fields up to 40 MV/m to **implant** positive and negative **charges** on the opposite **internal surfaces** of each cell, which behaves like a **dipole**
- The resulting cellular PDMS films show an **elastic modulus** of at least **21% lower** than solid ones and a **piezoelectric coefficient** (d_{33}) up to **182 pC/N**, which is about **10 times higher** than that of common piezoelectric polymers (e.g., **PVDF**)



Operating Principle

- The **charging** of the cells is realized by placing cellular PDMS films in **strong electric fields**, which eventually cause the **air inside** the cells to **break down**
- Upon the application of **mechanical or electrical stresses**, the **quasi-dipoles** inside PDMS films change their **dimensions and dipole moments**, which results in the desired **piezoelectricity**

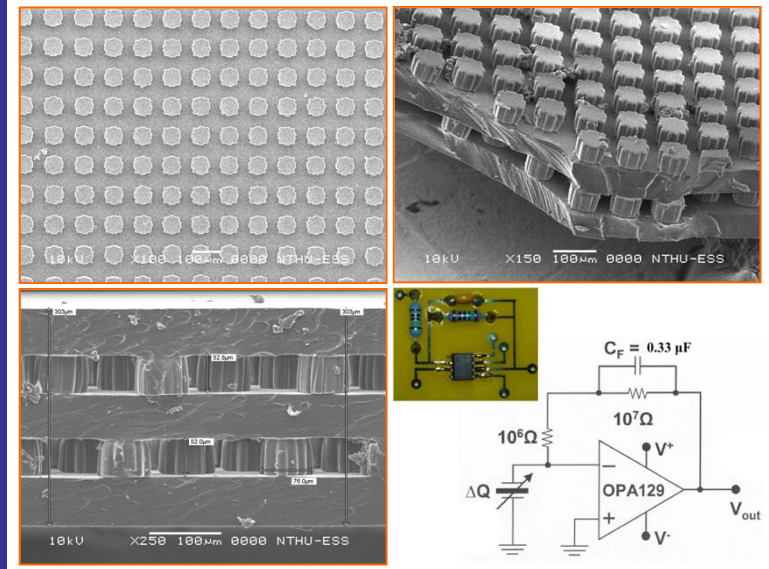


Fabrication

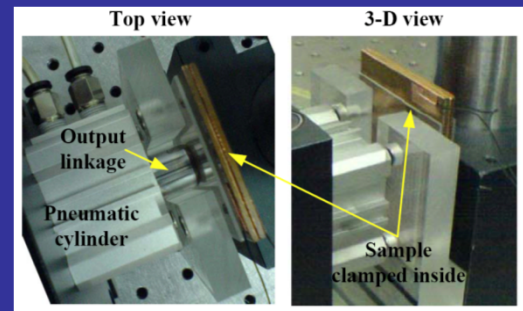
- Casting, stacking, and micro plasma discharge** processes are utilized
- Both **closed** and **open** cell structures were fabricated and characterized
- With **open** cell structures, **surface deposition** can be realized to include **extra semi-crystalline polymers** or **dielectric nanoparticles**, which are capable of storing charges stably and therefore improving the piezoelectricity
- Charge voltages were triangular waves with amplitude between 1 and 10 KV and frequencies of less than 0.2 Hz, while the charged PDMS films were heated up to 140 °C

Results

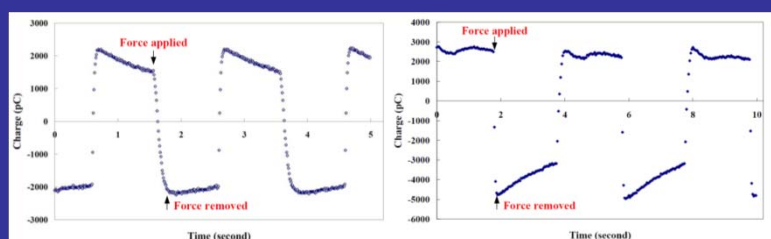
- Stacks of **two layers of inner cells** with overall thickness about **250 ~ 300 μm** were formed



- A **40 N** force, which corresponds to an air pressure of **1 kgf/cm²**, was applied on each of the **3 cm × 3 cm** large tested sample
- The elastic modulus of the open-cell type sample is **21% lower** than the solid ones



- Open cell:** The application of a 40 N force results in a **4120 pC** charge variation, which corresponds to a piezoelectric coefficient (d_{33}) of **103 pC/N**
- Closed cell:** The application of a 40 N force results in a **7310 pC** charge variation, which corresponds to a piezoelectric coefficient (d_{33}) of **182 pC/N**, about 10 times higher than that of common piezoelectric polymers (e.g., PVDF)



Acknowledgement

This work is supported by the National Science Council of Taiwan (**NSC 99-2628-E-007-028**)

國科會補助計畫衍生研發成果推廣資料表

日期:2011/10/23

國科會補助計畫	計畫名稱：多功能微液滴操控平台與陣列式反應器系統的開發
	計畫主持人：蘇育全
	計畫編號：99-2628-E-007-028-學門領域：熱傳學、流體力學
無研發成果推廣資料	

99 年度專題研究計畫研究成果彙整表

計畫主持人：蘇育全			計畫編號：99-2628-E-007-028-				
計畫名稱：多功能微液滴操控平台與陣列式反應器系統的開發							
成果項目			量化			單位	備註（質化說明：如數個計畫共同成果、成果列為該期刊之封面故事...等）
			實際已達成數（被接受或已發表）	預期總達成數(含實際已達成數)	本計畫實際貢獻百分比		
國內	論文著作	期刊論文	0	0	100%	篇	
		研究報告/技術報告	2	3	80%		碩士論文
		研討會論文	0	0	100%		
		專書	0	0	100%		
	專利	申請中件數	0	0	100%	件	
		已獲得件數	0	0	100%		
	技術移轉	件數	0	0	100%	件	
		權利金	0	0	100%	千元	
	參與計畫人力（本國籍）	碩士生	4	4	100%	人次	
		博士生	1	1	100%		
		博士後研究員	0	0	100%		
		專任助理	0	0	100%		
國外	論文著作	期刊論文	2	3	80%	篇	Nanofluidics & Microfluidics and JMM
		研究報告/技術報告	0	0	100%		
		研討會論文	4	4	80%		MicroTAS and Transducers
		專書	0	0	100%	章/本	
	專利	申請中件數	0	0	100%	件	
		已獲得件數	0	0	100%		
	技術移轉	件數	0	0	100%	件	
		權利金	0	0	100%	千元	
	參與計畫人力（外國籍）	碩士生	0	0	100%	人次	
		博士生	0	0	100%		
		博士後研究員	0	0	100%		
		專任助理	0	0	100%		

<p>其他成果</p> <p>(無法以量化表達之成果如辦理學術活動、獲得獎項、重要國際合作、研究成果國際影響力及其他協助產業技術發展之具體效益事項等，請以文字敘述填列。)</p>	無
---	---

	成果項目	量化	名稱或內容性質簡述
科教處計畫加填項目	測驗工具(含質性與量性)	0	
	課程/模組	0	
	電腦及網路系統或工具	0	
	教材	0	
	舉辦之活動/競賽	0	
	研討會/工作坊	0	
	電子報、網站	0	
	計畫成果推廣之參與（閱聽）人數	0	

國科會補助專題研究計畫成果報告自評表

請就研究內容與原計畫相符程度、達成預期目標情況、研究成果之學術或應用價值（簡要敘述成果所代表之意義、價值、影響或進一步發展之可能性）、是否適合在學術期刊發表或申請專利、主要發現或其他有關價值等，作一綜合評估。

1. 請就研究內容與原計畫相符程度、達成預期目標情況作一綜合評估

☒達成目標

☐未達成目標（請說明，以 100 字為限）

☐實驗失敗

☐因故實驗中斷

☐其他原因

說明：

2. 研究成果在學術期刊發表或申請專利等情形：

論文：☒已發表 ☐未發表之文稿 ☐撰寫中 ☐無

專利：☐已獲得 ☐申請中 ☒無

技轉：☐已技轉 ☐洽談中 ☒無

其他：（以 100 字為限）

初步成果已經發表在三篇碩士學位論文，四篇國際研討會論文(MicroTAS and Transducers)，以及三篇 SCI 期刊論文(Nanofluidics & Microfluidics and JMM)。透過逐步建立的基礎，陸續將有更多更有價值的成果可以被發表於 SCI 期刊與國際會議。

3. 請依學術成就、技術創新、社會影響等方面，評估研究成果之學術或應用價值（簡要敘述成果所代表之意義、價值、影響或進一步發展之可能性）（以 500 字為限）

快速樣本製備與反應條件篩選技術的發展將會為生化檢驗相關研究帶來多方面的衝擊。以本計畫主要的應用領域，奈米粒子與觸媒合成、蛋白質晶體成長與分析、藥物與細胞/微生物包埋、以及生醫檢測等應用而言，在生活上生醫檢測所需的時間可以被縮短，檢查的項目可以增加，在產業上材料或藥物的開發週期將可以被有效的縮減，成本可以大幅降低，並且迅速的累積在藥物設計與測試等各方面的經驗。在學術上，新技術將可以取代目前一般實驗室中所使用，以人工處理樣本，既緩慢又會消耗大量載具與樣本的實驗程序，有效的加速實驗流程、降低成本、擴展研究範圍，並且提升實驗的整體效能。初步成果已經發表在三篇碩士學位論文，四篇國際研討會論文(MicroTAS and Transducers)，以及三篇 SCI 期刊論文(Nanofluidics and Microfluidics and JMM)。透過逐步建立的基礎，投入人力進行深入研究，陸續將有更多更有價值的成果可以被發表於 SCI 期刊與國際會議。